



Active behavior of the Cytoskeleton

F. Jülicher^a, K. Kruse^{a,b}, J. Prost^{c,d}, J.-F. Joanny^{c,*}

^aMax-Planck Institut für Physik komplexer Systeme, Nöthnitzerstr. 38, 01187 Dresden, Germany

^bTheoretische Physik, Universität des Saarlandes, Postfach 151150, 66041 Saarbrücken, Germany

^cInstitut Curie, UMR CNRS 168, 26 rue d'Ulm 75248 Paris Cedex 05, France

^dE.S.P.C.I., 10 rue Vauquelin, 75231 Paris Cedex 05, France

Available online 28 March 2007

editor: I. Procaccia

Abstract

This review presents some of our recent results on active polar gels. Active polar gels are viscoelastic materials formed by polar filaments which are maintained in a non-equilibrium state by constant consumption of energy. This non-equilibrium state is characterized by the existence of internal stresses and spontaneous flows. A defining example of an active polar gel is provided by the acto-myosin cytoskeleton of eukaryotic cells. It is formed by actin filaments interacting with myosin molecular motors which are driven by the hydrolysis of adenosine-tri-phosphate (ATP).

We first present a hydrodynamic theory of active polar gels. The hydrodynamic equations are generic as they only rely on symmetry arguments. We then use the hydrodynamic approach to study the spontaneous generation of flow in an active polar film and the formation of vortex defects. The last part of this review is devoted to an analysis of the active gel theory in situations which are reminiscent of structures formed by the cytoskeleton in living cells.

© 2007 Elsevier B.V. All rights reserved.

PACS: 87.10.+e; 87.17.Jj; 82.70.Gg

Contents

| | |
|--|----|
| 1. Introduction | 4 |
| 2. Simple examples of active gels | 5 |
| 2.1. Passive actin gel growing on a curved surface: treadmilling and viscoelasticity | 5 |
| 2.2. Thin active gel layer: active stress | 8 |
| 3. Constitutive equations of active polar gels | 10 |
| 3.1. Polar order in active gels | 10 |
| 3.2. Linear hydrodynamic description of active polar gels | 10 |
| 3.3. Rotational viscoelasticity | 12 |
| 3.4. Beyond the simple linear one fluid description | 13 |
| 3.4.1. Permeation effects | 13 |
| 3.4.2. Non-linear couplings | 13 |
| 3.4.3. Active and passive noise | 14 |
| 4. Spontaneous flow of active gels | 14 |
| 4.1. Flow induced by boundary conditions | 14 |

* Corresponding author.

E-mail address: jean-francois.joanny@curie.fr (J.-F. Joanny).

| | |
|---|----|
| 4.2. Spontaneous Frederiks transition | 16 |
| 5. Vortices in active gels | 16 |
| 5.1. Topological defect of charge one in active films | 17 |
| 5.1.1. Topological defects in a passive system | 17 |
| 5.1.2. Spiral defects in an active system | 18 |
| 5.2. Dynamic phase diagram of compressible active films | 19 |
| 6. Active gel theory and the cell cytoskeleton | 21 |
| 6.1. Lamellipodium motion | 21 |
| 6.2. Relaxation modes of the cytoskeleton and wave propagation | 23 |
| 6.3. Polymerization limited by active stress in a flat geometry | 24 |
| 7. Concluding remarks | 25 |
| Acknowledgments | 26 |
| References | 26 |

1. Introduction

The mechanical properties of cells play an important role in many fundamental cellular processes such as adhesion, motility and division [1–3]. From a mechanical point of view, the cell is a soft elastic material with an elastic modulus in the range of 10^3 Pa. In a first approximation, these mechanical properties are determined by the cytoskeleton, a network of filamentous proteins. There are three different kinds of cytoskeletal filaments, microtubules, actin filaments, and intermediate filaments. As long as the cell is only weakly deformed, though, its response is mostly determined by the actin cytoskeleton alone. A description of the cellular processes mentioned before thus requires a physical theory of the actin cytoskeleton.

Actin is a globular protein that can assemble into a filamentous structure [1]. In these actin filaments two proto-filaments wind around each other and form a right-handed helix. Due to the structural properties of globular actin, actin filaments are endowed with a polar structure. The two different ends are, respectively, referred to as plus- (or barbed) and as minus- (or pointed) end. Under usual physiological conditions, actin filaments are out of equilibrium as they are treadmilling: globular actin is added at the plus- and dissociates from the minus-end. This process is driven by the hydrolysis of adenosine-tri-phosphate (ATP) during which chemical energy is released while ATP splits up into adenosine-di-phosphate (ADP) and inorganic phosphate P_i . In fact, actin associates with the plus-end of a filament when bound to ATP, while dissociation from the minus-end occurs after ATP-hydrolysis when actin is bound to ADP.

In a cell, actin filaments interact with a whole range of proteins [4]. In particular, some proteins cross-link actin filaments. Proteins like fascin or villin, lead to the formation of filament bundles, for example, in microvilli or stereocilia. Other proteins like filamin cross-link actin filaments without imposing a relative orientation on the linked filaments. This leads to an actin gel, the actin structure that is dominant in a living cell.

Generally, polymer gels are cross-linked networks formed by linear or branched polymers [5]. One distinguishes between chemical and physical gels. In a chemical gel, cross-links are established by covalent bonds. For all practical purposes they have an infinite lifetime, such that a chemical gel is a solid with a finite shear modulus at long times in the range of 10^3 – 10^6 Pa. On the contrary, in physical gels, cross-links are formed by physical interactions such as dipolar interactions, ionic bonds or by a local crystallization. These cross-links have a short lifetime (typically minutes, seconds, or still shorter). Consequently, a physical gel is viscoelastic. On short time scales it behaves like a solid with a finite shear modulus, but on long time scales it behaves like a liquid with a finite viscosity. Polymer physics provides good microscopic models to study the elasticity or the viscoelasticity of both, physical and chemical gels [6,7].

It is thus tempting to consider the actin cytoskeleton as a classical physical gel. However, this ignores the fact that the actin cytoskeleton is an active material: it is not an equilibrium system but it continuously consumes energy in the form of ATP. As we have already mentioned, ATP hydrolysis is involved in actin treadmilling. In addition, it is responsible for the activity of myosin II. Myosin II is a non-processive motor protein which transforms the chemical energy released in the course of ATP hydrolysis into mechanical work [3]. Small myosin II aggregates (mini-filaments) can cross-link several actin filaments and thereby generate stresses in the actin network [8]. Experimentally, these internal stresses are found to contract the actin gel [9,10]. A physical description of the cell cytoskeleton must thus take into account the viscoelasticity of the actin gel, the polar nature of the filaments, the treadmilling process, and the actively generated

stress due to ATP consumption. The aim of this review is to describe our recent work on a hydrodynamic theory of active polar gels and to present some applications of this theory to cellular problems.

Many theoretical works on the cytoskeleton start from microscopic considerations at the molecular level and show how the interactions between actin filaments and molecular motors can lead to the active behavior observed on macroscopic scales. This, of course, requires a good knowledge at the molecular level of both actin filaments and myosin motors. Kruse and Jülicher [11–13] have proposed a model for the dynamics of actin bundles which leads to an expression for the tension inside the bundle and to a prediction of bundle instabilities. Marchetti and Liverpool [14,15] as well as others have extended this approach to higher dimensions and studied in particular instabilities of the isotropic homogenous filament distribution. To this end effective descriptions on macroscopic scales were derived from the microscopic equations. In contrast to this approach, the hydrodynamic theory which we present here, starts on macroscopic scales.

As for classical hydrodynamics, our description is independent of many of the microscopic details governing the evolution of the system. Instead it depends on a number of phenomenological parameters analogous to the viscosity of simple fluids. The physical behavior of the system essentially depends on the values of these parameters, which have to be determined experimentally or which might be obtained from microscopic theories. The structure of the hydrodynamic equations is imposed by the symmetries of the system studied and is therefore universal [16,17]. This approach has been successfully applied to many systems, e.g., biological membranes [18], vibrated sand piles [19], self-propelled colloidal objects [20,21], bacterial colonies [22] as well as bird flocks [23]. These theories have, in particular, revealed the existence of propagative waves with finite propagation velocity in active systems which we call Ramaswamy waves [24]. The main limitation of the hydrodynamic theory is that it considers only large length scales and long time scales. In an actin gel, for example the hydrodynamic theory can only describe the properties of the gel at length scales larger than the mesh size.

The review is organized as follows. In the next section we give two simple examples, which illustrate the two original properties of the cytoskeleton, treadmilling and active stresses. We first discuss the growth of an actin gel in the absence of myosin motors on a curved surface. In this situation, which is relevant for recent bio-mimetic experiments on the bacterium *Listeria Monocytogenes*, only treadmilling and viscoelasticity of the actin gel play a role. The second example is that of thin active gel of constant thickness. This essentially one-dimensional geometry allows for a simple introduction of active stresses in the theory. In Section 3, we give the general equations of the hydrodynamic theory of active polar gels. Here, we do not give the systematic derivation of these equations, which can be found in Refs. [25,26]. Rather, we point to the differences between active polar gels and other hydrodynamic systems such as nematic liquid crystals, gels, or passive viscoelastic materials (physical gels). We also discuss the limits of this approach and possible improvements of the theory. In Section 4, we show that an active gel can spontaneously flow in the presence of a polarization gradient. A passive liquid or elastic gel would not flow in such a situation. Section 5 is devoted to topological defects of the polarization field and their possible biological relevance. We first discuss a single defect that can be a vortex, an aster or a spiral and then the stability of a thin active film, in particular, with respect to the appearance of defects. In Section 6, we give some applications of the theory of active gels to cellular processes. Finally, the last section presents some concluding remarks and discusses some further issues.

2. Simple examples of active gels

In this section, we illustrate some of the important features of the hydrodynamics of active gels: treadmilling, viscoelasticity and active contraction. We do not refer to the general hydrodynamic equations, which will be presented in the next section, but discuss two examples that allow for a simpler treatment. First, we treat the growth of an actin gel in a curved geometry. This process plays a major role in problems related to *Listeria*-like motility, for which treadmilling and viscoelasticity of the cytoskeleton are important. The second example illustrates the importance of active contractions. Here, we discuss the motion of a thin gel layer of constant thickness, which is an extremely simplified model for lamellipodium motion.

2.1. Passive actin gel growing on a curved surface: treadmilling and viscoelasticity

The bacterium *Listeria Monocytogenes* provides one of the simplest examples of cell motility [27]: On its surface, the bacterium polymerizes actin of the host cell, which eventually leads to the formation of a comet. As a consequence of adding new material at the bacterial surface, the previously formed actin gel is deformed, which results in elastic

forces propelling the bacterium within the host cell. No molecular motors like myosin are involved in this process and the gel can be considered as passive (although, as mentioned above, ATP hydrolysis is required for treadmilling of actin). Furthermore, the polarity of actin does not seem to play a major role and one can consider the actin comet as an isotropic gel. Depolymerization occurs in the bulk of the comet and at its rear.

Many bio-mimetic experiments have been devised to study quantitatively *Listeria*-like motility [28]. In these experiments, colloidal objects of various shapes (spherical and cylindrical or planar solid objects [29], oil drops [30], vesicles [31,32]) are coated with proteins promoting actin polymerization and are immersed either in a cell extract or in a solution of a few (as low as 5) purified proteins. At first, a gel grows uniformly around the object. Then, there is a spontaneous symmetry breaking in the gel which leads to the formation of a comet [33,34]. The comet grows at a velocity similar to that of *Listeria* motion which is of the order of micrometers per minute.

Let us describe uniform growth of a gel [35]. We consider the gel as a viscoelastic material with a single viscoelastic relaxation time τ and a short time shear modulus E [36,37]. The simplest mechanical model to describe viscoelasticity is the so-called Maxwell model. In this model, the deviatoric stress $\sigma_{\alpha\beta}$ is related to the strain rate tensor (the velocity gradient) $v_{\alpha\beta} = \frac{1}{2}(\partial_\alpha v_\beta + \partial_\beta v_\alpha)$, where v_α is the velocity field in the gel, by

$$\frac{\partial \sigma_{\alpha\beta}}{\partial t} + \frac{\sigma_{\alpha\beta}}{\tau} = 2E v_{\alpha\beta}. \quad (1)$$

At times smaller than the viscoelastic relaxation time τ , the gel behaves as an elastic solid with shear modulus E , while at long times it behaves as a liquid with finite viscosity $\eta = E\tau$. Typical orders of magnitude are $E = 10^3$ Pa, $\tau = 10$ s and $\eta = 10^4$ Pa s [38]. This constitutive equation is not invariant under Galilean transformations. However, in the growing gel of the comet, each material element is convected by treadmilling due to the polymerization on the surface of the cylinder. It is therefore essential to have a Galilean invariant form in order to take into account treadmilling. This can be achieved by replacing in Eq. (1) the partial derivative with respect to time by a convected derivative $d/dt = \partial/\partial t + \mathbf{v} \cdot \nabla$, where \mathbf{v} is the local velocity in the gel. Note, that the constitutive equation is still not rotationally invariant. Other terms are added in Section 3 to ensure invariance under rotations. They play no role here and can be ignored. Note furthermore, that the convected derivative introduces geometric non-linearities. There could also exist other non-linear terms in the constitutive equation involving, for example, the square of the strain or of the stress tensors. In the rest of this paper, though, we ignore these non-linearities of the material and, in exactly the same spirit as in liquid crystal physics, we retain the geometrical non-linearities (associated here to the convected derivative, which describes the treadmilling process).

The limit of a purely elastic comet, which is usually used to describe the *Listeria* comet, is obtained with an infinite relaxation time τ . Note, however, that even the dynamics of an elastic comet is not a classical continuum elasticity problem: the boundary condition on the surface does not give neither the strain nor the stress on the surface. Instead, the velocity is imposed by polymerization. This is a hydrodynamic boundary condition for an elasticity problem. An alternative way to study this problem is to come back to the definition of the strain in the gel by defining locally a metric tensor (called the Finger tensor in rheology) and consider its variation in space. The viscoelastic formulation that we discuss here turns out to be much simpler.

In the following, we consider the uniform growth of a gel around a cylinder¹ of radius R , see Fig. 1.

The gel thickness is h and we use cylindrical coordinates (r, θ) , while there is no dependence on the z coordinate along the cylinder axis. Furthermore, we ignore the depolymerization in the bulk of the gel [27] and we consider the gel as incompressible so that $\nabla \cdot \mathbf{v} = 0$. This is a reasonable approximation for actin gels which have a Poisson modulus close to 0.5. The trace of the stress tensor $\sigma_{ii} = \sigma_{rr} + \sigma_{\theta\theta}$ then vanishes and the pressure field P in the gel ensures incompressibility. In a cylindrical geometry, only two components of the stress tensor, the radial component σ_{rr} and the ortho-radial component $\sigma_{\theta\theta}$, do not vanish and the velocity v only depends on the distance r to the axis of the cylinder. The local force balance in the radial direction is written as

$$\frac{d\sigma_{rr}}{dr} + \frac{\sigma_{rr} - \sigma_{\theta\theta}}{r} = \frac{dP}{dr}. \quad (2)$$

¹ Very similar results are obtained for spherical growths, only numerical prefactors are different.

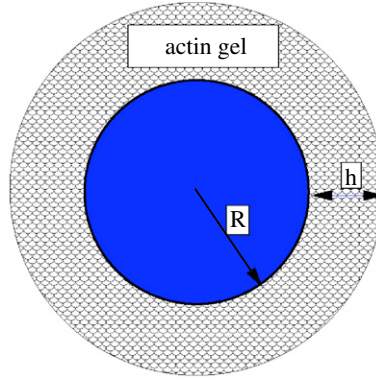


Fig. 1. Sketch of an actin gel growing around a cylinder of radius R . The equilibrium thickness of the gel h is reached when polymerization on the cylinder surface exactly compensates depolymerization on the outer surface.

In a steady state, the two constitutive equations of the convected Maxwell model are

$$v \frac{d\sigma_{rr}}{dr} + \frac{\sigma_{rr}}{\tau} = 2E \frac{dv}{dr}, \quad (3)$$

$$v \frac{d\sigma_{\theta\theta}}{dr} + \frac{\sigma_{\theta\theta}}{\tau} = 2E \frac{v}{r}. \quad (4)$$

The incompressibility condition imposes the variation of the velocity as a function of r , $v = v_p R/r$, where we have used the fact that, on the surface of the cylinder, the velocity is equal to the polymerization velocity v_p . The two components of the stress can then be calculated from the Maxwell constitutive equations and the pressure field from the force balance equation. At the free surface of the gel, $r = R + h$, the normal stress is continuous and $[\sigma_{rr} - P](R + h) = 0$. On the surface of the cylinder, the stress is fixed by the polymerization conditions. For simplicity, we suppose that when actin is polymerized, there is no tensile stress and that $[\sigma_{\theta\theta} - P](R) = 0$.

At lowest order in $1/R$ we obtain the components of the total stress as a function of the distance u from the cylinder surface ($r = R + u$):

$$\sigma_{\theta\theta} - P = \frac{4\eta v_p}{R} (1 - e^{-u/v_p \tau}), \quad (5)$$

$$\sigma_{rr} - P = \frac{4\eta (v_p \tau)^2}{R^2} \left(\frac{u - h}{v_p \tau} + e^{-u/v_p \tau} - e^{-h/v_p \tau} \right). \quad (6)$$

As expected, at short distance $u < \lambda_e = v_p \tau$ from the surface, the stress is purely elastic and depends only on the elastic shear modulus E . At larger distances, the stress is mostly viscous.

If we assume that depolymerization occurs only at the surface of the growing gel with a depolymerization velocity v_d the variation of the gel thickness with time is such that

$$\frac{dh}{dt} = v(R + h) - v_d \simeq v_p - v_d. \quad (7)$$

The depolymerization velocity increases with the ortho-radial stress on the gel surface $[\sigma_{\theta\theta} - P](R + h)$. Kramers rate theory [39,40] suggest an exponential increase $v_d = v_d^0 \exp \{[\sigma_{\theta\theta} - P](R + h)/\sigma_0\}$. As the thickness h increases, the depolymerization velocity increases and becomes equal to the polymerization velocity at the steady-state thickness

$$h = -v_p \tau \log \left(1 - \frac{\sigma_0 g R}{4E \tau v_p} \right), \quad (8)$$

where $g = \log v_p/v_d^0$ is a dimensionless polymerization free energy.

In the purely elastic regime where $\alpha = \sigma_0 g R/4E \tau v_d \ll 1$, the gel thickness is proportional to the radius and increases as $h/R = \sigma_0 g/4E$. This is the result already found in Ref. [40] in a spherical geometry (where the only difference is

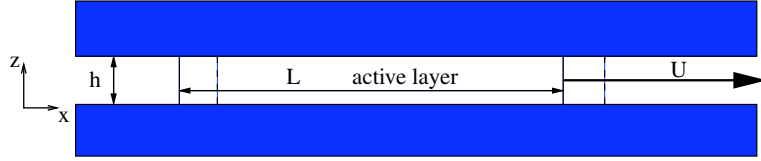


Fig. 2. Thin gel layer in a slab. The layer advances at a velocity U . It polymerizes at the front and depolymerizes at the back. The adhesion on the lower surface is described by a viscous friction law. There is no adhesion on the upper surface.

that the numerical prefactor 4 is replaced by 6). The thickness increases strongly with α when viscous effects become important and diverges for $\alpha = 1$. A more detailed study of the gel growth including the diffusion of actin monomers and a comparison to the experimental results can be found in Ref. [27].

2.2. Thin active gel layer: active stress

In contrast to *Listeria*-like motility, the locomotion of most other cells requires the presence of motor proteins. An example is provided by crawling cells that adhere to a solid substrate. In this case, the cell body is pulled forward by forces generated in a sheet-like protrusion in the front of the cell. This protrusion, called lamellipodium, is filled with actin cytoskeleton. Using a drug to isolate fragments from lamellipodia of fish keratocytes, Euteneuer and Schliwa [41] have shown that fragments by themselves are motile. These fragments are essentially sheets of actin filaments, molecular motors and proteins, which regulate actin assembly and disassembly, surrounded by a membrane. Subsequent studies by Verkhovsky et al. [8] on fragments have yielded spectacular results on cell motility, e.g., the ability of the cytoskeleton to self-organize into a moving state. In order to show effects of actively generated stresses in the cytoskeleton, we now discuss a very simple model of fragment locomotion [26].

Consider a thin sheet of active gel of constant height h and length L moving on a solid substrate in the (x, y) -plane (see Fig. 2). The velocity is oriented in the x -direction and has a magnitude U . For simplicity, we assume that the gel properties are invariant in the direction y . Cell or fragment motion is only possible if momentum is transferred to the environment, for example, through adhesion to a substrate. Adhesion of a cell or a fragment on a solid substrate is known to occur via adhesion protein links which are continuously broken and rebuilt [42]. This complex adhesion process can be described by a friction stress proportional to the local velocity $\sigma_{xz} = \xi v$ [43], where ξ is an effective friction coefficient and z denotes the direction perpendicular to the substrate, see Fig. 2. Here, as in the following, all velocities are expressed in the reference frame of the substrate.

We consider a small slice of gel of length dx and thickness h . For simplicity, we only consider adhesion on the lower surface of the gel and we assume a free boundary condition on the upper surface of the gel. The gel on the right and on the left of this section exerts a force σh along the x -axis, where $\sigma = (1/h) \int_0^h dz \sigma_{xx}$ is the average of the tensile stress over the gel thickness. The substrate exerts a friction force $\sigma_{xz} dx$. The force balance on this small slice of gel can therefore be written as

$$\frac{d}{dx} h \sigma = \xi v. \quad (9)$$

The stress σ_{xx} and the velocity v in x -direction do not vary much over the gel thickness. We thus employ a thin film approximation and neglect their dependence on z . This reduces the study of the thin gel motion to a one dimensional problem. Note, that the assumption of a constant thickness implies that we consider the gel as fully compressible. A more realistic description is given in Section 6. We now need a constitutive equation relating the stress σ to the velocity gradient.

As in the case of *Listeria*-like motility, we describe the actin gel as a viscoelastic material with an elastic modulus E and a viscoelastic relaxation time τ . Myosin II transform chemical energy derived from the hydrolysis of ATP into mechanical work which generates contractile stresses in the actin network. On a phenomenological level, we take this active effect into account by adding a constant “active” stress. In a linear theory, the active stress is proportional to the energy produced by ATP or to $\Delta\mu$, the chemical potential difference between ATP and its hydrolysis products. We thus write the active stress as $\zeta \Delta\mu$, where ζ is a material parameter of the cytoskeleton characterizing motor activity. For a

systematic justification of this expression we refer to the next section. The constitutive equation for the active gel in the reference frame of the substrate is then written as

$$2\eta \frac{\partial v}{\partial x} = \sigma + \tau \left(\frac{\partial \sigma}{\partial t} + v \frac{\partial \sigma}{\partial x} \right) + \zeta \Delta \mu. \quad (10)$$

Here, we use ζ as a phenomenological parameter, which must be obtained from experiments. Though its value has not been measured, it was shown that motor activity leads to contractility such that $\zeta < 0$ [9,10]. Alternatively, its value might be obtained from single molecule properties by using a microscopic model, such as those described in [11–15]. In a keratocyte, Myosin II forms small aggregates [8]. A simple guess then is that the motors generate active stress by forming active cross-links between different filaments. For small motor concentrations c_m , this idea leads to $\zeta \sim -c_m c_f^2$, where c_f is the density of actin monomers in the gel.

We now discuss the steady state of a cell layer of length L advancing along the x -direction at constant velocity U . Combining the force balance equation (9) with the constitutive equation (10), we obtain an equation for the stress inside the gel layer. In the laboratory reference frame, the stress is a function of $(x - Ut)$ and

$$\lambda^2 \frac{d^2 \sigma}{dx^2} = \sigma + \tau \left(\frac{h}{\xi} \frac{d\sigma}{dx} - U \right) \frac{d\sigma}{dx} + \zeta \Delta \mu, \quad (11)$$

where the friction length λ is defined as $\lambda^2 = 2h\eta/\xi$. It is useful to measure the stress in units of $-\zeta\Delta\mu$, defining $\sigma = -\tilde{\sigma}\zeta\Delta\mu$ and the velocities in units $(|\zeta\Delta\mu|h)/\lambda\xi$ defining $U = \tilde{U}(|\zeta\Delta\mu|h)/\lambda\xi$. In addition to the advancing velocity \tilde{U} , the stress equation (11) is thus seen to depend on a second dimensionless parameter $\beta = \tau|\zeta\Delta\mu|/2\eta$. Elastic terms can be ignored if $\beta \ll 1$ and become dominant if $\beta \gg 1$. In the following, we suppose in agreement with the existing data that $\beta \ll 1$ and that the gel is not submitted to any external force. Therefore, at the front, $x = L$, and at the rear, $x = 0$, the stress vanishes $\sigma = 0$. The stress and velocity distributions are then given by

$$\sigma = -\zeta\Delta\mu \left(1 - \frac{\cosh((2x - L)/2\lambda)}{\cosh L/2\lambda} \right), \quad (12)$$

$$v = \frac{\zeta\Delta\mu h}{\lambda\xi} \frac{\sinh((2x - L)/2\lambda)}{\cosh(L/2\lambda)}. \quad (13)$$

Because of the contractile effect of the gel, the stress is positive. If $L \gg \lambda$ it is approximately constant in the center of the gel and decays to zero over a length λ . The velocity field is symmetric. The velocity vanishes in the center of the gel, it is negative over a length λ at the front, $x = L$, and the flow is retrograde; it is positive over a length λ at the back and the flow is anterograde. Note that in this scenario, the velocity of the material elements in the reference frame of the substrate is independent of the polymerization and depolymerization conditions and that it is only driven by the active stress. An essential assumption of this very simple model is that the gel is perfectly compressible so that there is no pressure gradient in the force balance equation. A more realistic description of an incompressible gel is given below in Section 6.1.

The average velocity U of the gel layer is determined by filament polymerization and depolymerization. In the simplest model, the gel polymerizes at the front with a polymerization velocity v_p and depolymerizes at the back with a depolymerization velocity v_d . The boundary conditions for the velocity are thus $U = v(L) + v_p = v(0) + v_d$. These two conditions fix the gel advancing velocity $U = (v_p + v_d)/2$ and the length of the gel such that $-(2\zeta\Delta\mu h/\lambda\xi) \tanh(L/2\lambda) = v_p - v_d$.

As the velocity is positive at the back and negative at the front, mass conservation imposes that the density of the gels grows towards the rear. For a gel with a finite compressibility the thickness does not remain constant and increases towards the rear.

The main message of this simple example is that the existence of an active stress is sufficient to induce a velocity field inside the gel that tends to contract the gel. We have considered here the limit of a purely viscous gel, but, as in the previous section, at the front of the gel, where polymerization occurs, there exists a region of size $\lambda_e \sim -\tau\zeta\Delta\mu h/\lambda\xi$, where the gel has a solid-like behavior and the velocity is nearly constant. Note that the viscous behavior that we discussed is observed if $\lambda_e < \lambda$. In the opposite limit, the gel has a solid-like behavior.

3. Constitutive equations of active polar gels

We now turn to the general constitutive equations for the hydrodynamics of an active polar gel [25,26]. In the examples treated in the previous section, the polar nature of actin filaments entered only through the boundary conditions. In general, though, it will also affect the dynamics in the bulk of the material. We therefore start our presentation with a discussion of the polar order.

3.1. Polar order in active gels

On each actin filament, we define locally a unit vector in the direction from the minus end to the plus end. The local polarization field \mathbf{p} is defined as the average of the unit vectors in a small volume around each point. The thermodynamics of the polarization field can be studied from the standard free energy of polar nematic liquid crystals or ferro-electric liquids [44]:

$$\mathcal{F} = \int d\mathbf{r} \left[\frac{K_1}{2} (\nabla \cdot \mathbf{p})^2 + \frac{K_2}{2} (\mathbf{p} \cdot (\nabla \times \mathbf{p}))^2 + \frac{K_3}{2} (\mathbf{p} \times (\nabla \times \mathbf{p}))^2 + k \nabla \cdot \mathbf{p} - \frac{h_{\parallel}^0}{2} \mathbf{p}^2 \right]. \quad (14)$$

The three Frank constants K_i for splay, twist, and bend are positive. The coefficient k describes the spontaneous splay allowed by the vector symmetry of the polarization field. This term does not exist for a non-polar nematic liquid crystal, which in our case corresponds to parallel actin filaments with a random orientation.

The field conjugate to the polarization field is defined as $\mathbf{h} = -\delta\mathcal{F}/\delta\mathbf{p}$. It has a component h_{\parallel} parallel to the local polarization \mathbf{p} , which controls the amplitude of the local polarization, i.e., the local degree of orientation of the actin filaments. The parallel component of the field includes the field h_{\parallel}^0 in Eq. (14) but it also eventually includes a contribution from the Frank elastic free energy. In the following, we consider the limit where orientation fluctuations dominate and amplitude fluctuations as small. This implies that the modulus p of the polarization is constant and can be chosen equal to 1 without loss of generality. The parallel field can in this case be regarded as a Lagrange multiplier which ensures this constraint. The field also has a transverse component h_{\perp} . According to the free energy given in Eq. (14), the transverse field creates a torque that tends to align the polarization field.

In the following we are mostly interested in the thin active gels that form the cell cytoskeleton, for example, in a lamellipodium. This is a quasi-two-dimensional system and in most cases, the polarization field can be considered as two dimensional in the plane of the film. For a two-dimensional polarization field, the twist deformations are not possible and there are only two Frank constants $K_1 = K$ and $K_3 = K + \delta K$. A simple approximation is the one-constant approximation where the anisotropy δK vanishes. This simplifies the theoretical description, but it is probably not justified for actin filaments.

3.2. Linear hydrodynamic description of active polar gels

In order to build up a linear hydrodynamic theory of the cytoskeleton, we follow closely the lines proposed by Martin, Parodi and Pershan for the hydrodynamic theory of nematic liquid crystals [16]. We identify the fluxes and forces and we write the most general linear relation between them, which respects the symmetry of the problem. The hydrodynamic description is a macroscopic theory in the sense that it applies to length and time scales much larger than any molecular scale. On these scales, we do not need to consider the precise mechanisms of energy consumption, i.e., we do not need to take into account the details of the mechanisms underlying the action of molecular motors. They are captured by the values of the phenomenological parameters, called Onsager coefficients, present in the theory. Here, we consider them as given material properties of the cytoskeletal system, which must be measured separately.

As a first approximation, we consider the active polar gel as an effective one component system. The quantities that we take as fluxes are the mechanical stress $\tilde{\sigma}_{\alpha\beta}$, which is associated with the mechanical properties of the gel, the rate of change of the polarization $\dot{\mathbf{P}}$, and the rate of consumption of ATP per unit volume r .

The generalized force conjugate to the ATP consumption rate is the chemical potential difference $\Delta\mu$ between ATP and its hydrolysis products, i.e., the free energy gained per hydrolyzed ATP molecule. The force conjugate to the rate of change in the polarization is the field \mathbf{h} and the force conjugate to the stress tensor is the velocity gradient tensor $\partial_{\alpha}v_{\beta}$.

We define locally the velocity \mathbf{v} of the center of mass of each volume element that we consider to define the velocity field. The velocity gradient tensor at a point \mathbf{r} can be decomposed into a symmetric part $\tilde{v}_{\alpha\beta} = \frac{1}{2}(\partial v_\alpha/\partial r_\beta + \partial v_\beta/\partial r_\alpha)$ and an antisymmetric part $\omega_{\alpha\beta} = \frac{1}{2}(\partial v_\alpha/\partial r_\beta - \partial v_\beta/\partial r_\alpha)$ which describes the vorticity of the flow. For the following, it is useful to separate the traceless part of the tensor and to define $v_{\alpha\beta} = \tilde{v}_{\alpha\beta} - \frac{1}{3}\tilde{v}_{\gamma\gamma}\delta_{\alpha\beta}$.

Similarly, we decompose the total deviatoric stress tensor $\tilde{\sigma}_{\alpha\beta}$ into an isotropic part $-p = \frac{1}{3}\tilde{\sigma}_{\gamma\gamma}$, which is a contribution to the pressure in the gel, and a traceless part $\sigma_{\alpha\beta}^t = \tilde{\sigma}_{\alpha\beta} - \frac{1}{3}\tilde{\sigma}_{\gamma\gamma}\delta_{\alpha\beta}$. For a non-isotropic material, the stress tensor is not symmetric and can be decomposed into a symmetric part and an antisymmetric part. We write the traceless component of the stress tensor as $\sigma_{\alpha\beta}^t = \sigma_{\alpha\beta}^a + \sigma_{\alpha\beta}$. The antisymmetric part of the stress tensor describes the torque acting on each volume element. As for a nematic liquid crystal, it is given by [44]

$$\sigma_{\alpha\beta}^a = \frac{1}{2}(p_\alpha h_\beta - p_\beta h_\alpha). \quad (15)$$

The phenomenological linear dynamic equation relating the stress to the velocity gradient and all the other forces must respect all the symmetries of the polar gel. First, there is only one vector in the problem, the polarization \mathbf{p} , and one traceless second-order tensor, namely the quadrupolar or nematic tensor. If locally all actin filaments are parallel, its components are $q_{\alpha\beta} = p_\alpha p_\beta - \frac{1}{3}p^2\delta_{\alpha\beta}$. Note, that if the actin gel is not polar but has nematic order, the average value of the polarization vanishes but the average value of the quadrupolar tensor does not vanish. A second important symmetry is the time-reversal symmetry. It allows to distinguish between the dissipative component of a flux, which is associated with energy dissipation, and its reactive or elastic component. Taking all symmetries into account, the general equation for the traceless part of the stress then reads [25,26]

$$2\eta v_{\alpha\beta} = \left(1 + \tau \frac{D}{Dt}\right) \left\{ \sigma_{\alpha\beta} + \zeta \Delta\mu q_{\alpha\beta} + \tau A_{\alpha\beta} - \frac{v_1}{2} \left(p_\alpha h_\beta + p_\beta h_\alpha - \frac{2}{3} h_\gamma p_\gamma \delta_{\alpha\beta} \right) \right\}. \quad (16)$$

As in the previous section, we use the dynamics of the convected Maxwell model with a single viscoelastic relaxation time τ [36,37]. In order to ensure the invariance with respect to translation and rotation, the convected time derivative must be replaced by the co-rotational derivative $(D/Dt)\sigma_{\alpha\beta} = (\partial/\partial t + v_\gamma\partial/\partial r_\gamma)\sigma_{\alpha\beta} + [\omega_{\alpha\gamma}\sigma_{\gamma\beta} + \omega_{\beta\gamma}\sigma_{\gamma\alpha}]$. Recent experiments show that the rheological properties of the cytoskeleton are not captured by a single viscoelastic relaxation time, but require a broad distribution of relaxation times (a power law distribution) [45,46]. As the theory is linear, the distribution of relaxation times could be introduced by considering Maxwell models with different relaxation times in parallel. This makes the theory more complex and it has not been considered yet. In the following, we only consider the Maxwell model with a single relaxation time τ , which represents the longest relaxation time in the system, and a shear viscosity η . The tensor $A_{\alpha\beta}$ describes geometrical nonlinearities, which we do not wish to discuss here. These non-linearities are included in the so-called ‘‘Oldroyd eight constant model’’, which is a classical generalization of the convected Maxwell model for the properties of viscoelastic fluids.

In addition to the viscosity, the stress equation involves two other reactive parameters. The coefficient v_1 describes the coupling between the mechanical stress and the polarization field. This is a well-known parameter in liquid crystal hydrodynamics and several experiments have been built to measure it for classical liquid crystals. We are not aware, though, of any measurements of its value for actin. An important result from liquid crystal hydrodynamics is that instabilities occur if $|v_1| < 1$.

The important new parameter is the coefficient of active stress generation ζ that we have already introduced phenomenologically in the previous section. It couples the activity in the system, measured by the difference in chemical potential $\Delta\mu$, to the stress. The active coefficient can be positive corresponding to a dilational stress or negative corresponding to a contractile stress. All experimental results point into the direction that the internal stress in the cytoskeleton is contractile; we therefore use a negative value of ζ in the following. It is important to note the quadrupolar symmetry of the active stress. This symmetry is associated with a normal stress difference, i.e., with a different value of the normal stress acting on planes oriented in different directions.

Considering the active gel as incompressible, which seems to be a good approximation for actin gels, the isotropic part p of the stress tensor plays no role; it can be incorporated in the pressure and only the total pressure is meaningful as a Lagrange multiplier ensuring incompressibility of the system. For a compressible system, the pressure p must be added to the thermodynamic pressure. It satisfies an equation very similar to the traceless part of the stress tensor

that we give here for completeness

$$\bar{\eta} \tilde{v}_{\alpha\alpha} = \left(1 + \tau \frac{D}{Dt}\right) \{-p + \bar{\zeta} \Delta\mu + \tau A - \bar{v}_1 h_\gamma p_\gamma\}. \quad (17)$$

We have introduced here longitudinal Onsager coefficients, which play the same role as the transverse coefficients introduced in the equation for the traceless part of the stress tensor.

Let us now turn to the second flux. The rate of change of the polarization is defined as $\dot{\mathbf{P}} = D\mathbf{p}/Dt$. As for the stress, we must use the co-rotational convected time derivative of the polarization vector given by $(D/Dt)p_\alpha = \partial p_\alpha / \partial t + (v_\gamma \partial_\gamma) p_\alpha + \omega_{\alpha\beta} p_\beta$. The Onsager relation for the polarization reads

$$\frac{D}{Dt} p_\alpha = \frac{1}{\gamma_1} h_\alpha + \lambda_1 p_\alpha \Delta\mu - v_1 v_{\alpha\beta} p_\beta - \bar{v}_1 v_{\beta\alpha} p_\beta. \quad (18)$$

In this equation, the rotational viscosity γ_1 characterizes dissipation due to rotation of the polarization. It has units of a standard viscosity and is always positive. The rotational viscosity has been measured for classical liquid crystals and for polymeric liquid crystals, but we do not know of any results for actin gels or semi-dilute solutions. The coupling between the polarization and the mechanical stress is described by the same coefficients v_1 and \bar{v}_1 as in the stress equations (16) and (17). The signs of the associated terms in Eq. (18) are imposed by the Onsager symmetry relations. The only new coefficient associated with the activity is the coefficient λ_1 . It corresponds to an active field which tends to drive the actin filaments parallel (if λ_1 is positive, which is not imposed by thermodynamics, though). Several models [47–50] for this effect have been built based on the torques exerted by molecular motor aggregates on the actin filaments.

The final Onsager relation gives the rate of consumption of ATP:

$$r = A \Delta\mu + \zeta p_\alpha p_\beta v_{\alpha\beta} + \bar{\zeta} v_{\alpha\alpha} + \lambda_1 p_\alpha h_\alpha. \quad (19)$$

The diagonal coefficient A measures the rate of consumption of ATP in the absence of velocity gradient and polarization field. The non-diagonal coefficients account for the coupling between ATP consumption and, respectively, mechanical stress and polarization changes. As for the polarization equation, they are imposed by the Onsager symmetry relations.

In Eqs. (16) and (18) for the stress and the polarization, there are only two terms that depend on the activity. They are proportional to $\Delta\mu$ with corresponding material parameters ζ and λ_1 , respectively. Note, however, that if the polarization has a fixed modulus, the parallel field is a Lagrange multiplier which is determined by imposing the modulus of the polarization. In this case, one can define an effective longitudinal field $\tilde{h}_\alpha = h_\alpha + \gamma_1 \lambda_1 p_\alpha$. This effective field has the same perpendicular component as the original field and a modified parallel component which is itself determined by the modulus of the polarization. Using this effective field, there remains only one active term in the stress equation, where ζ is replaced by the effective parameter $\tilde{\zeta} = \zeta + \lambda_1 v_1 \gamma_1$.

The constitutive equations (16), (18), and (19) are generic equations respecting the vectorial symmetry of the polarization and of time-reversal symmetry. Note, that we have ignored here the chirality of the actin filaments, which would introduce additional terms with a chiral asymmetry. The choice of the constitutive equation for the stress in absence of activity and polarization, i.e., the convected Maxwell model, however, is not imposed by the symmetries of the problem, but guided by physical results: this is the simplest viscoelastic model with liquid-like behavior at long and solid-like behavior at short times. A natural generalization of the Maxwell model would be to introduce a distribution of relaxation times [45,46]. As mentioned above this is necessary to describe some recent experiments. We have also assumed that the rotation of the polarization is only associated with viscous dissipation. This is certainly a good approximation at long times when the active gel flows. In this limit, our equations reduce to the hydrodynamic equations of polar nematic liquid crystals. At short times, one expects an elastic response of the polarization, which is not captured by Eq. (18). We now discuss this rotational viscoelasticity.

3.3. Rotational viscoelasticity

In this section, we introduce viscoelasticity of the polarization dynamics using the same level of description that we have used for the flow equation. There are no constraints on the viscoelastic behavior imposed by the symmetries and we must rely on a phenomenological description. We use a model with a single relaxation time similar to the Maxwell model or the Debye model of dielectrics. Moreover, we choose the same relaxation time for the rotational and

translational motion of the filaments. In the cytoskeleton, actin filaments are strongly entangled and the local rotations of the polarization are hindered by the entanglement constraints. Therefore, relaxation can only occur by a reptational worm-like motion of the filaments. The longest relaxation time both for rotational and translational motion is thus the disengagement or rotation time. We use it here as a parameter and refer to the book of Doi and Edwards for a more precise discussion [51].

As for the stress, we want to impose the behavior of the polarization in the absence of activity and in the limits of short and long times. For long times, the gel flows and has the same hydrodynamics as polar nematic liquids, see above. At short times, we expect an elastic behavior and the rheological equations must reduce to that of a nematic (polar) gel. The elasticity of nematic gels and the coupling between the deformation field and the director field have been studied in details both experimentally and theoretically. General references are the book of Warner and Terentjev [52] or the work of Finkelmann and coworkers [53]. We do not discuss this complex problem here, we only give the viscoelastic polarization equation obtained in Ref. [54] which has the correct short time behavior. Note that this equation

$$\frac{Dp_\alpha}{Dt} = \frac{1}{\gamma_1} \left(1 + \tau \frac{D}{Dt} \right) h_\alpha + \lambda_1 p_\alpha \Delta \mu - v_1 v_{\alpha\beta} p_\beta + \bar{v}_1 v_{\beta\beta} p_\alpha \quad (20)$$

is different from the one proposed in Refs. [25,26].

3.4. Beyond the simple linear one fluid description

3.4.1. Permeation effects

In a first step, we have modeled the acto-myosin system as a single component active polar gel. This is a strong approximation as the cytoskeleton is clearly a multi-component system including both polymerized and monomeric actin, both, free motors and motors bound to actin, and the cytosol, which is itself composed by the solvent water and a large number of proteins.

A systematic derivation of the linear hydrodynamic equations for a multi-component active polar gel will be given in the forthcoming reference [55]. The theory, however, is more complex and involves a large number of Onsager coefficients. This goes beyond the scope of the present review and we only wish to describe here the main qualitative features that do not exist in the one-component description.

The most important qualitative effect which is neglected in the one-component fluid description is permeation. The multi-component hydrodynamic theory essentially reduces to the one-component theory presented above if there is no relative motion between the gel and the cytosol. The permeation through the gel can be an important source of dissipation that is not always negligible.

A typical example where permeation plays a role is given by the simple thin gel model discussed in Section 2.2. As polymerization occurs only at the front of the gel, new gel is formed ahead of the advancing gel fragment. This new gel is swollen by the cytosol which requires a permeation flow of the cytosol through the already existing gel.

In a multi-component system, the relevant velocity is the center of mass velocity and one must also introduce the relative fluxes \mathbf{j}^i of all the components with respect to the center-of-mass of each volume element. The flux \mathbf{j}^i of a component i of concentration c^i and chemical potential μ^i contains a convective part, a diffusion part and couples to both, the active terms and the polarization. If we ignore the coupling to polarization, we can write

$$j_\alpha^i = c^i v_\alpha - A^{ij} \partial_\alpha \mu_j + \kappa^i p_\alpha \Delta \mu. \quad (21)$$

The mobility tensor A^{ij} is not diagonal because of the hydrodynamic coupling between components in a rather dense solution. The diagonal mobility A^{ii} is proportional to the diffusion constant of component i . The mobility tensor can also be anisotropic and contain terms proportional $p_\alpha p_\beta$ leading to different diffusion constants in different directions.

The active term of the bound motors is related to their velocity v_m along actin filaments $\kappa_m \Delta \mu = c_m \mathbf{v}_m$. Note, that this is a polar term that does not exist for a system with nematic symmetry. The other currents are also coupled to the activity. The origin and the importance of these couplings are discussed in Ref. [55].

3.4.2. Non-linear couplings

A second limitation of the simplest active gel hydrodynamic theory is the restriction to linear terms in the constitutive equations. The only non-linearities are of a geometrical origin. The linear approach is systematic: once the choice of

fluxes and forces has been made, the symmetries impose the structure of the theory and relations between the Onsager coefficients. The only freedom of the theory is the rheological model for which we have chosen here the Maxwell model with a single relaxation time.

This linear approach is valid only in the vicinity of thermodynamic equilibrium. Biological systems are rarely close to equilibrium and the linear theory is in most instances not sufficient. In a second step, the expansion could be extended to second order, that is, to use relations between the fluxes and the forces including quadratic terms in $\Delta\mu$, in the field \mathbf{h} , or in the velocity gradient. This approach, although systematic, would be impractical because it requires the introduction of a too large number of non-linear terms.

We favor here a different approach, where we use the generic linear approach and we introduce some non-linearity only when new physics is needed. The choice of these non-linearities must, of course, be guided by experimental results. In doing so, we lose part of the general and systematic character of the theory. Let us illustrate this approach by two examples.

In Section 2.1, we have studied the formation of a passive active gel around a spherical colloidal object. One of the essential ingredients of our approach is the fact that the depolymerization velocity rapidly increases with the tensile stress in the gel. A linear theory would assume that the depolymerization velocity increases linearly with the tensile stress. Bio-mimetic systems for *Listeria* show that this would be in strong disagreement with experiments. Kramers theory [39,56] of chemical reactions, as well as recent experiments with the so-called Bio-membrane force probe [57] support the exponential variation with stress that we use.

A second example concerns the active stress. The strict linear theory imposes that the active coefficient ζ is a constant as the active stress is already first order in $\Delta\mu$. Any comparison with a molecular theory will lead to an active coefficient depending on both, the gel density c_f and the bound motor density c_m . As we have argued above, a naive guess is $\zeta \sim -c_m c_f^2$. In the linear theory, the concentrations must be replaced by their average values in the active gel. The linear theory therefore neglects gradients of activity in the gel. Experimentally, however, it is known that the density of molecular motors in cells is not homogeneous. Molecular motors are for example known to accumulate at the rear of lamellipodia [8]. The ensuing gradient of activity can control some important physical properties such as the propagation of waves or the thickness of cortical actin discussed below. In order to describe these phenomena, one must go beyond the linear theory.

3.4.3. Active and passive noise

The active gel theory of Section 3.2 only considers the average values of the physical quantities and ignores their fluctuations. The noise in active gels has in general a non-thermal nature. Close to thermal equilibrium, thermal noise can also play a role.

Thermal noise is related to the linear response of the gel to external perturbations by the fluctuation dissipation theorem. Its effects can therefore be calculated directly from the equations of the linear hydrodynamic theory. A detailed study of the effects of thermal noise in active gels will be given in Ref. [58]. It leads to results very similar to those obtained in the theory of active nematic liquid crystals: the fluctuations in the polarization field strongly influence the diffusion of a small particle in the active gel and can lead to a renormalization of both, the viscosity and the elastic modulus of the gel.

Active noise in the gel can be due to the stochasticity in the polymerization, due to the stochastic motor activity or due to active processes for example in the cell membrane. The study of active noise represents a big challenge because of the lack of systematic approaches. Active noise has been discussed for so-called active membranes [18,59] for which it strongly modifies the fluctuation spectrum and for mechano-sensory hair cells of the ear [60].

4. Spontaneous flow of active gels

In this section, we give two examples where the spontaneous flow of a thin active polar film is driven by a polarization gradient. In the first example the polarization gradient is externally imposed while in the second example, it spontaneously appears above a certain film thickness.

4.1. Flow induced by boundary conditions

Consider a film of thickness L on a solid substrate. The film is parallel to the (x, y) -plane and we assume that the properties of the film are translationally invariant in the (x, y) -plane along the y -direction so that the problem is

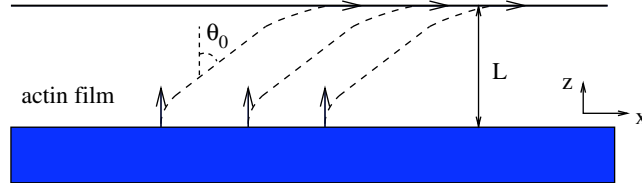


Fig. 3. Active film on a substrate with mixed anchoring conditions. The actin filaments are parallel to the free surface of the film but they are perpendicular to the solid surface.

essentially two-dimensional as shown in Fig. 3. The free surface of the film is at $z=L$ and the solid surface at $z=0$. The orientation of the polarization is measured by the angle θ with the z -axis perpendicular to the film surface. We consider the case where at $z=L$ the polarization is parallel to the free surface ($\theta(L) = \pi/2$) while at $z=0$ it is perpendicular to the solid surface ($\theta(0) = 0$).

In the case of an incompressible film, the velocity v_z in the direction perpendicular to the film vanishes. Under these conditions, both, the polarization angle θ and the velocity v in the x -direction, depend only on z . The constitutive equations for the stress (16) lead to [61]

$$\sigma_{xz} + \frac{\zeta \Delta \mu}{2} \sin 2\theta - \frac{v_1}{2} (h_{\parallel} \sin 2\theta + h_{\perp} \cos 2\theta) = 2\eta u, \quad (22)$$

$$\sigma_{zx}^a + \frac{h_{\perp}}{2} = 0, \quad (23)$$

where $u = \frac{1}{2} dv/dz$ is the velocity gradient. In a steady state, the equations for the polarization (18) read

$$u v_1 \sin 2\theta = \frac{h_{\parallel}}{\gamma_1} + \lambda_1 \Delta \mu, \quad (24)$$

$$u (v_1 \cos 2\theta - 1) = \frac{h_{\perp}}{\gamma_1}. \quad (25)$$

The equation of force balance $\partial_{\beta} \sigma_{\alpha\beta} - \partial_{\alpha} P = 0$ along the z direction imposes that σ_{zx} is independent of z . Therefore, it vanishes everywhere as it vanishes on the free surface. The constitutive equations can be combined to a single equation for the polarization angle:

$$\partial_z^2 \theta = \frac{\tilde{\zeta} \Delta \mu \sin 2\theta (v_1 \cos 2\theta - 1)}{K [4(\eta/\gamma_1) + v_1^2 - 2v_1 \cos 2\theta + 1]}. \quad (26)$$

This equation can be integrated once leading to $\frac{1}{2} (\partial_z \theta)^2 = -E(\theta)$, where $E(\theta)$ is an effective potential energy. This energy has minima for $\theta = 0, \pi/2$ and a maximum at the angle θ_0 such that $\cos 2\theta_0 = 1/v_1$.

In the case of a thick film, the polarization angle is close to θ_0 except in the vicinities of the surfaces. We can then expand the effective energy around θ_0 : $E(\theta) = E(0) - (1/2\xi^2)(\theta - \theta_0)^2$, where the decay length of the polarization is defined as $\xi^{-2} = (-2\tilde{\zeta}\Delta\mu/v_1 K)(v_1^2 - 1)/(4(\eta/\gamma_1) + v_1^2 - 1)$. In the limit, where the film thickness is large compared to ξ , there are two boundary layers of thickness ξ on each side of the film where the polarization angle relaxes exponentially to the value θ_0 . In the center of the film, the polarization angle is constant and equal to θ_0 . Over most of the film the velocity gradient, Eq. (25), is constant and equal to $u = \tilde{\zeta}\Delta\mu \sin 2\theta_0 / \gamma_1 [4(\eta/\gamma_1) + v_1^2 - 1]$. For $\tilde{\zeta}\Delta\mu < 0$, u is negative. Because the velocity vanishes on the solid surface $z=0$, the velocity is everywhere directed towards negative values of x . There is therefore a finite flux of liquid

$$Q = \int_0^L dz v(z) = \frac{\tilde{\zeta} \Delta \mu \sin 2\theta_0}{\gamma_1 [4(\eta/\gamma_1) + v_1^2 - 1]} L^2/2. \quad (27)$$

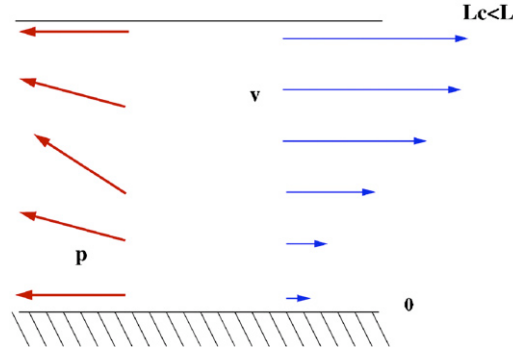


Fig. 4. Gel on a solid substrate and the associated flow. The gel thickness L is larger than the Frederiks transition threshold L_c .

4.2. Spontaneous Frederiks transition

As in the previous section, we consider again a thin film, but now with a boundary condition, such that the polarization is parallel to the x -direction on both surfaces. Then, there is a static steady state of the film with $\mathbf{v} = 0$, and a constant polarization parallel to the x -direction. Here, we study the stability of this steady-state solution [61].

As in the previous section, we consider a free surface at $z=L$ and a solid substrate at $z=0$. The constitutive equations are thus the same as in the previous section and the total transverse stress $\bar{\sigma}_{z,x}$ vanishes on the surfaces of the film.

We consider a perturbation of the static state, where the polarization angle is slightly tilted and θ only weakly deviates from $\pi/2$; we write $\theta = \pi/2 - \epsilon$. Expanding Eq. (26), the tilt ϵ is a solution of

$$\partial_z^2 \epsilon + \frac{\pi^2}{L_c^2} \epsilon = 0, \quad (28)$$

where $L_c^2 = -\pi^2 K (4\eta/\gamma_1 + (v_1 + 1)^2) / 2\tilde{\zeta}\Delta\mu(v_1 + 1)$. If the active stress is contractile ($\tilde{\zeta} < 0$), then L_c^2 is indeed positive and L_c is a well-defined length.

If the thickness L of the active film is smaller than L_c , then the only solution to Eq. (28) which satisfies the boundary conditions $\epsilon(0) = \epsilon(L) = 0$ is $\epsilon = 0$. The polarization thus remains parallel to the x -direction and there is no flow in the film. At the critical value of the thickness $L = L_c$, there is a bifurcation and the tilt of the polarization becomes finite. If L is close to the critical value, the polarization angle behaves as $\epsilon = \epsilon_m \sin(\pi z/L)$. The amplitude ϵ_m cannot be calculated from the linear theory proposed here and requires the calculation of the non-linear terms. Beyond the bifurcation, the amplitude varies as $\epsilon_m \sim \pm(L - L_c)^{1/2}$. Note, that there are two possible tilts of the polarization in opposite directions, and the symmetry is spontaneously broken. This transition is similar to the classical Frederiks transition of nematic liquid crystals, where a tilt of the director orientation imposed by surfaces is due to an external magnetic field [44]. There is no magnetic field here and the tilt results from the active stresses. The new feature of the active film is that above the transition, the velocity field does not vanish. It is given by $v = [4L\tilde{\zeta}\Delta\mu\epsilon_m/\pi(4\eta + \gamma(v_1 + 1)^2)](\cos(x\pi/L) - 1)$. The velocity has everywhere the same sign and there is a finite flux of liquid in the x -direction. Note, that the flux can occur either in the positive or in the negative direction depending on the sign of the polarization tilt even though the film is polar. The polarization field in the gel and the associated flow are displayed in Fig. 4.

A similar Frederiks transition occurs with different hydrodynamic boundary conditions. For a film confined between two solid surfaces, the velocity vanishes on both surfaces of the film. The transition between a static and a flowing state occurs at a thickness $L = 2L_c$ and there is no net flux of liquid in the x -direction.

We have supposed here that the free surface of the film remains flat corresponding to a high surface tension and we have only considered distortion of the polarization in the (x, z) -plane. Distortions in the (x, y) -plane are also possible and lead to another type of instability that has been recently studied by Ramaswamy [62].

5. Vortices in active gels

Actin filaments have a persistence length of the order of $15 \mu\text{m}$ and tend to align at least locally to form a phase with polar order or in some cases a nematic phase [3]. In most instances, the polarization varies smoothly in space

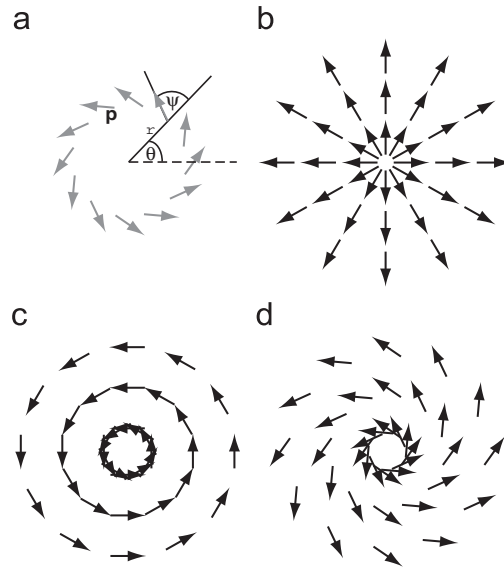


Fig. 5. Possible point defects of topological charge one in two dimensions. (a) Illustration of the definition of the angles θ and ψ . (b–d) The orientations of the polarization vectors are displayed as arrows for an aster (a), a vortex (b) and a spiral (c).

under the influence of external fields. However, the polarization can have a very strong variation, around a so-called topological defect of the polarization field. At this point, the polarization is not well-defined. In this section, we discuss the properties of such defects in thin active polar gels. We only consider polar gels in two dimensions, having in mind the very thin films formed by the actin network in cells. We first discuss an isolated defect of topological charge 1. We then discuss the stability of a thin film with respect to the formation of such defects.

5.1. Topological defect of charge one in active films

Before studying a topological defect of charge 1 in an active polar gel, it is useful to recall the properties of such defects in a passive system corresponding to a ferroelectric liquid or a polar nematic [44].

5.1.1. Topological defects in a passive system

We first use the one-constant approximation for the orientation free energy (14), $K_1 = K_3$, and impose a polarization of modulus $p = 1$. In a two-dimensional system, the polarization at point \mathbf{r} can then be characterized by its polar angle $\phi(\mathbf{r})$. The transverse field conjugate to the polarization is then $h_{\perp} = K \nabla^2 \phi$. In equilibrium, the transverse field vanishes and the polarization angle is such that

$$\nabla^2 \phi = 0. \quad (29)$$

The solution of this equation that corresponds to topological defects, that is, which is singular at the origin, can be written as $\phi = m\theta + \psi_0$, where we have used polar coordinates, ($\mathbf{r} = (r, \theta)$), and where ψ_0 is a constant, see Fig. 5a. The topological charge of the defect m is an integer; which counts the number of turns of the polarization while turning once around the defect. Note, that in contrast to nematic liquid crystals half-integer values of m are not allowed for polar systems. In the following, we focus on topological defects of charge $m = 1$. The possible defects are shown in Fig. 5b–d.

If $\psi_0 = 0, \pi$, then the defect is an aster with the polarization pointing either towards the origin or away from it. If $\psi_0 = \pi/2, -\pi/2$, then the defect is a vortex. For defects with any other value of ψ_0 , the polarization spirals around the origin. The equation of the spirals in polar coordinates is

$$r(\theta) = r_0 \exp[\theta \cot \psi_0]. \quad (30)$$

In the limit of isotropic Franck constants, $K_3 - K_1 = \delta K = 0$, all these defects have the same free energy and occur with the same probability. In the more realistic case with $\delta K \neq 0$, spirals are never stable. Asters are stable if $\delta K > 0$, when splay deformation is favored, and vortices are stable if $\delta K < 0$, when bend deformation is favored.

5.1.2. Spiral defects in an active system

We now consider a topological defect of charge 1 in an active incompressible system in the liquid limit where $\tau \rightarrow 0$ [25,26]. As above, we use polar coordinates and look for a rotationally invariant steady-state solution. The polarization angle is written as $\phi(r, \theta) = \theta + \psi(r)$. The incompressibility condition $\nabla \cdot \mathbf{v} = 0$ and the fact that the velocity must not have any singularity impose that the radial velocity vanishes, $v_r = 0$. The velocity field is thus ortho-radial and the only non-vanishing component of the strain rate tensor is $v_{r\theta} = \frac{1}{2} \partial v_\theta / \partial r$.

In steady state, the constitutive equation (18) for the rate of change of the polarization relates the components of the field \mathbf{h} to the strain rate tensor by

$$v_1 v_{r\theta} \sin 2\psi - \lambda_1 \Delta \mu = \frac{h_{\parallel}}{\gamma_1}, \quad (31)$$

$$(v_1 \cos 2\psi - 1) v_{r\theta} = \frac{h_{\perp}}{\gamma_1}. \quad (32)$$

The three components of the stress tensor $\tilde{\sigma}_{rr}, \tilde{\sigma}_{\theta\theta}, \tilde{\sigma}_{r\theta}$ depend only on the radius r . The force balance equation projected on the θ -direction reads $(1/r^2)(d/dr)(r^2 \tilde{\sigma}_{r\theta}) = 0$. It implies $\tilde{\sigma}_{r\theta} = 0$, because the stress cannot have a singularity at the origin. The symmetric part of the stress tensor is then

$$\sigma_{r\theta} = h_{\parallel}/2. \quad (33)$$

Combining Eqs. (33), (32) and the $(r\theta)$ -component of the constitutive equation (16) for the stress, we obtain an equation for the polarization angle

$$h_{\perp}(4\eta + \gamma_1 v_1 (v_1 - \cos 2\psi)) = \gamma_1 \sin 2\psi (v_1 \cos 2\psi - 1) \tilde{\zeta} \Delta \mu. \quad (34)$$

As above, we have introduced here the effective active stress coefficient $\tilde{\zeta} = \zeta + v_1 \gamma_1 \lambda_1$.

We now look for solutions of Eq. (16) to describe topological defects of charge one in an active system. If we first ignore the anisotropy of the Franck constants, $\delta K = 0$, then the only solutions of Eq. (16) with $h_{\perp} = 0$ are spirals with a constant angle $\psi = \psi_0$ such that

$$\cos 2\psi_0 = 1/v_1. \quad (35)$$

There is therefore a dynamic selection of the spirals. The selected angle is the same as the steady state angle of a nematic liquid crystal in a shear flow, relative to the shear axis. Note, that quite similarly to nematics in a shear flow, there is no steady state if $|v_1| < 1$. If $|v_1| \geq 1$, then the transverse component of the velocity gradient is $v_{r\theta} = \omega/2 = [\sin 2\psi_0 / (4\eta + \gamma_1 v_1^2 \sin^2 2\psi_0)] \tilde{\zeta} \Delta \mu$. The determination of the velocity field requires a boundary condition at large distances. Here, we choose the simple condition, that the velocity v_θ vanishes at a distance R from the center such that

$$v_\theta = \omega r \log r/R. \quad (36)$$

The whole spiral is thus rotating at a slowly varying angular velocity $\omega \log r/R$. Rotating spiral defects have been observed by Nédélec and coworkers in solutions of microtubules interacting with kinesin molecular motors. The theory that we describe here is generic and can be applied also to kinesin–microtubule mixtures [63–66].

So far, the actin gel has been considered as purely two dimensional. In many cases, though, the active film interacts with a substrate. As in Section 2.2, an interaction with the substrate can be described by a friction coefficient per unit area ξ , so that the force per unit area exerted by the substrate on the gel is $-\xi \mathbf{v}$. The effect of the friction force has been calculated in detail in Refs. [25,26]. It is characterized by a friction length $\lambda_f = ((4\eta + \gamma_1 v_1 \sin^2 2\psi_0) / 2\xi)^{1/2}$. At distances from the center of the defect smaller than λ_f , the effect of the substrate friction is negligible and the velocity is given by Eq. (36), where the friction length plays the role of the large length scale R . At larger distances, the dissipation is dominated by the substrate friction and the velocity decreases exponentially to zero.

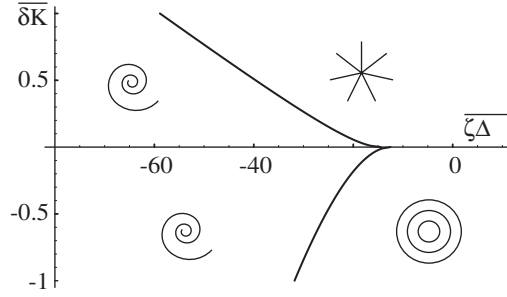


Fig. 6. Stability diagram of asters, vortices and spirals which are topological defects in an active gel of polar filaments. Asters are stable for $\delta K > 0$ in the region with actively generated stresses $\bar{\zeta\Delta\mu}$ larger than a critical value $\bar{\zeta\Delta\mu}_c^A$. This critical value is negative, corresponding to contractile stresses in the gel. Vortices are stable for $\delta K < 0$ and $\bar{\zeta\Delta\mu} > \bar{\zeta\Delta\mu}_c^V$. For other parameter values, rotating spirals occur via a symmetry breaking dynamic instability. Here, $\bar{\delta K} = \delta K/K$ is a dimensionless ratio of two elastic moduli and $\bar{\zeta\Delta\mu} = R^2\zeta\Delta\mu/K$ a dimensionless measure of active stresses. Note that both rotation senses occur with equal probability on symmetry grounds. The diagram was evaluated for the choice $\eta/\gamma_1 = 1$ and $\nu_1 = 2$ of Onsager coefficients of the system.

In the general case, the anisotropy of the Franck constants cannot be ignored. In the absence of activity, we have shown above that either vortices or asters are stable depending on the sign of the anisotropy δK . The stability of these defects has been studied in Refs. [25,26] as a function of the activity coefficient ζ . The stability diagram in the absence of substrate friction is displayed in Fig. 6. It shows the range of stability of the various defects in the plane $(\delta K, \zeta\Delta\mu)$ and reveals, that for a given value of δK , both, asters and vortices, are unstable if the activity is negative and large enough. This suggests that the stable defects are (rotating) spirals. In the system of microtubules and kinesins, a transition between asters and rotating spirals has been observed as the density of motors is increased [63–66]. This is in qualitative agreement with the phase diagram of Fig. 6 if we assume that both, the absolute value of the activity coefficient ζ and the Franck constant anisotropy δK , increase with the number of motors.

The role of topological defects in the actin polarization field has not been assessed fully for in vivo systems. In Ref. [25] it was proposed that the flow field of the cytoskeleton in moving keratocyte cells could be discussed based on a pair of point defects which rotate in opposite directions and are located on the two sides of the lamellipodium. In this scenario, each spiral defect creates a velocity field on the other spiral that transports the defect at a constant velocity forward. This drives the overall translational motion in a way similar to the motion of smoke rings. So far, there is no quantitative experimental evidence to support this simple picture. In vitro, as mentioned above, rotating spirals have been observed for microtubules interacting with kinesin motors. Recent experiments of the group of J. Käs on active actin films show the spontaneous appearance of complex structures [67,94]. Some of these structures look like aster or spiral defects. In the next section, we discuss the stability of active films and the appearance of defect structures.

5.2. Dynamic phase diagram of compressible active films

The aim of this section is to study the stability of thin active polar films. In the following, we average all properties over the thickness of the film and therefore discuss the film properties in two dimensions. Although the film itself is in general incompressible, the two-dimensional density $c(\mathbf{r})$ is not constant due to variations in the film thickness. We thus consider the film as a two-dimensional compressible system. Here, we only study small density fluctuations of the film around the average density c_0 , and write the local density as $c = c_0 + \rho$. The total free energy of the system \mathcal{F}_t is the sum the polarization free energy, Eq. (14), and a density-dependent contribution \mathcal{F}_d . For simplicity, we consider again the case of isotropic Franck constants and set $K_1 = K_3 = K$. The density-dependent contribution can be expanded up to second order in powers of ρ , $\mathcal{F}_d = \int d\mathbf{r}[w\rho\nabla \cdot \mathbf{p} + (\beta/2)(\nabla\rho)^2 + (\alpha/2)\rho^2]$. The compressibility α is positive and, together with the positive coefficient β , defines the correlation length $\xi_\rho = (\beta/\alpha)^{1/2}$ of density fluctuations. The coefficient w characterizes the coupling between density fluctuations and splay. Finally, the surface pressure in the film is $\Pi = c_0\delta\mathcal{F}_d/\delta\rho$.

The equations of motion of the film have two types of homogeneous steady states: static state where the velocity vanishes and the polarization is constant and dynamic steady states with a constant velocity gradient and a

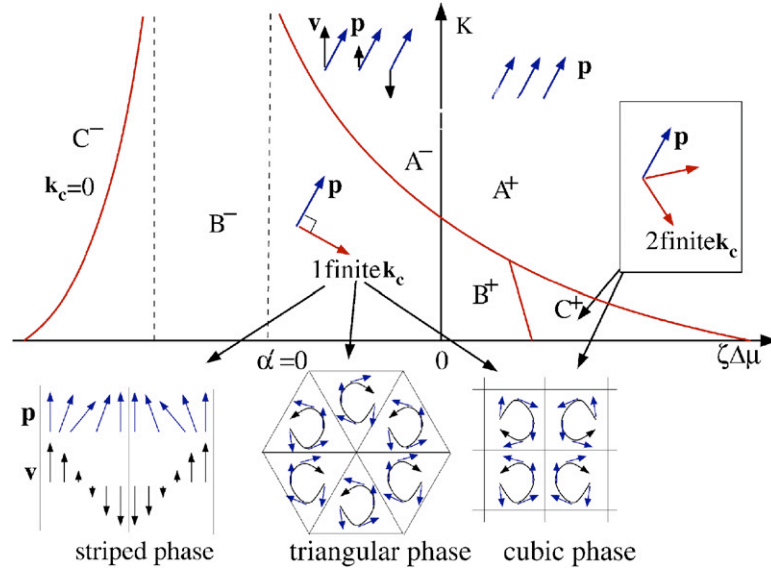


Fig. 7. Dynamic stability diagram of an active polar film. The various regions of the diagram are discussed in the text. We also show a sketch of the possible periodic structures.

constant polarization. In the dynamic steady state, the angle between the polarization and the velocity must satisfy Eq. (35).

In Ref. [68], we have studied the stability of the two types of steady states with respect to periodic perturbations with wave vector k using both analytical and numerical calculations. We have constructed a stability diagram in a $(K, \zeta\Delta\mu)$ -plane. The diagram is displayed in Fig. 7 in the limit of a vanishing active coefficient, $\lambda_1 = 0$.

Three regions can be distinguished in this diagram. In region A either the static or the dynamic homogenous steady state is macroscopically stable. In region A^- , the film spontaneously flows, quite similarly to what has been discussed in the previous section. In region C^- , both the static and the dynamic steady states are unstable with respect to a macroscopic perturbation (with a wave vector $k_c = 0$). In this range of parameters the activity coefficient ζ is negative and large, which corresponds to a strong contractility. The (renormalized) compressibility is then negative and one expects a macroscopic phase separation. This could correspond to the super-precipitation observed in actin–myosin systems [9,10,69,70] or to the formation of bundles by microtubules when the density of kinesin motors is increased.

In regions B and C^+ , at least one of the steady states is unstable with respect to periodic perturbations of finite wave vectors k_c . This instability is very similar to the instability described in Refs. [71,72] for passive nematics. In that case, the instability corresponds to the appearance of a periodic lattice of defects, which favors the apparition of splay. For the active system, this suggests a similar lattice of defects. Because of the existence of polarization gradients in this phase, the velocity gradient cannot vanish and the system flows locally. The symmetry of the phase cannot be inferred from the linear stability analysis and requires a non-linear analysis. One could expect either a lamellar phase or a hexagonal phase. The hexagonal phase, for example, corresponds to an ordered array of rotating spirals similar to those described in the previous paragraph. Finally, in region C^+ there are two independent unstable modes and this could correspond to an oblique phase of defects. Note, that the existence of an instability at a finite wave vector is not a proof of the existence of a periodic phase (as illustrated for example in the case of spinodal decomposition).

To date there exist no systematic studies of the dynamic phase diagram of actin–myosin films. However, both, simulations and some experiments, show the existence of phase separation and of disordered vortex phases with flow. We suggest here the existence of a flowing phase of ordered vortices. A disordered or glassy vortex phase could also exist as a metastable state and be stabilized by the intrinsic noise of the system.

The active gel theory can be applied to any type of active system sharing the same symmetries as the cytoskeletal gel. An example is bacterial suspensions. Recent experiments on two-dimensional bacterial colonies show flow patterns consisting of disordered rotating eddies of swimming bacteria [22]. This bacterial turbulence could also be a disordered

version of the mesophases suggested by our theory. The work of Ramaswamy and coworkers for hydrodynamically interacting self-propelled particles also predicts a flow instability [20,21]. This instability is different, though, from the one discussed here since there is no instability threshold. This difference might be due to the fact that our model only considers a one component compressible gel. A more detailed comparison between the two approaches would require the determination of the dynamic phase diagram using the multi-component active gel model outlined above.

6. Active gel theory and the cell cytoskeleton

In this section, we discuss applications of the active gel theory to some problems of cell biophysics. First, we discuss the actin flow in lamellipodia of cells crawling on a substrate and determine the height profile of these protrusions. It follows a study of propagating waves in active gels. Indeed, waves propagating at constant velocity seem to be a general feature of active systems and have been observed under various circumstances in the actin cytoskeleton of cells adhering to a substrate. Finally, we show how the active gel approach can be used to discuss physical properties of the cortical actin layer present in animal and many other cells.

6.1. Lamellipodium motion

The advancing velocity of a keratocyte cell has been measured to be of the order of $10 \mu\text{m}/\text{min}$. In the front region of the lamellipodium, the actin gel exhibits a retrograde flow with respect to the substrate measured in the reference frame of the substrate [73]. At the rear of the lamellipodium, close to the cell body the actin velocity changes sign and the flow is anterograde. On the sides of the cell, the flow field is more complex.

In order to discuss the actin dynamics in a lamellipodium as well as the associated height profile, we extend and modify the model presented in Section 2.2 [74]. For simplicity, we consider again a two-dimensional geometry. The motion is assumed to be directed along the x -axis and the height is measured in the z -direction. The velocity u of the lamellipodium is directed towards negative x -values. In the following, we choose the origin of the x -axis to coincide with the front of the lamellipodium, see Fig. 8. We furthermore assume that the polarization is fixed inside the lamellipodium with modulus one and pointing into the direction of motion.

Actin polymerization is promoted by proteins, such as Wiscott Aldrich Syndrom Proteins (WASP) family proteins which activate the ARP 2/3 complex. This complex generates branching of actin filaments and thus promotes the formation of new uncapped ends which can polymerize and thus extend the gel [75–78]. We assume here that the WASPs are located in the vicinity of the front and that their density is $\rho_{\text{wa}} = \rho_0 \exp(-x/\lambda)$ where the length scale λ is of the order of $1 \mu\text{m}$. We consider that actin polymerization occurs only on the cell surface and in the direction normal to the surface. The polymerization velocity \mathbf{v}_p is then given by $\mathbf{v}_p = k_p \rho_{\text{wa}}(x) \mathbf{n}$, where \mathbf{n} denotes the local normal to the cell surface and k_p the polymerization rate. In contrast to the treatment in Section 2.2, we consider here an incompressible actin gel and work in the limit where the slope of the lamellipodium height profile $h(x)$ is small, $|dh/dx| \ll 1$.

As above, we describe the effects of adhesion of the lamellipodium to the substrate by a viscous friction law, such that the transverse stress at the substrate surface is proportional to the local velocity, i.e., $\sigma_{zx} = \xi v(z=0)$, where ξ

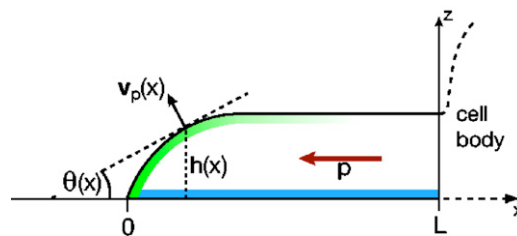


Fig. 8. Schematic representation of the two-dimensional geometry of a thin gel layer corresponding to a lamellipodium of a moving cell. The height profile $h(x)$ of the gel is described as a function of the distance x from the leading end of the lamellipodium. The lamellipodium length is denoted L . The gel in a lamellipodium is structurally polar with filaments pointing their plus ends towards the leading end of the lamellipodium. This polarization is described by the vector p . Polymerization of new gel material occurs at the surface of the gel layer in a direction normal to the surface and with velocity $v_p(x)$.

has dimensions of friction per unit area. The stress distribution below a moving keratocyte has been measured in [79]. Using this result and the velocity field reported in [73], we estimate the value of ξ to be $\xi \simeq 10^{10}$ Pa s/m.

The force balance in the gel is given by

$$\frac{\partial(h(\sigma - P))}{\partial x} = \xi v, \quad (37)$$

where the gel velocity v is measured in the reference frame of the substrate. In the thin film limit, the stress and the velocity depend only weakly on the transverse coordinate and can thus be considered as constant in the z -direction. The stress σ entering Eq. (37) is the average with respect to the thickness of the gel layer of the longitudinal component of the stress tensor σ_{xx} , $\sigma = (1/h) \int_0^h dz \sigma_{xx}$. Eq. (37) is very similar to Eq. (9), but we have now taken into account, that the cytoskeleton is incompressible and that its thickness $h(x)$ varies with the distance from the front. By writing the continuity of the normal stress at the upper surface of the gel, one obtains that $\sigma_{zz}(h) = P = -\sigma$ so that $\sigma - P = 2\sigma$. We first consider that the cytoskeleton is fluid and take the liquid limit of the constitutive equation (16). The stress averaged over the thickness of the film is then related to the velocity gradient by $2\eta \partial v / \partial x = \sigma + \zeta \Delta \mu$. Combining this equation with the force balance (37), we obtain a relation between the velocity v and the film thickness h .

In order to obtain both, the height profile of the lamellipodium and the gel velocity, we use the conservation of matter. In the moving reference frame of the lamellipodium, the flux of actin is $j_a = h(u + v)$. If, for simplicity, we neglect depolymerization in the bulk, then the variation of this flux is due to the polymerization, so that

$$\frac{\partial h(u + v)}{\partial x} = \rho_{wa}(x) k_p. \quad (38)$$

We consider here that the transition between the lamellipodium and the cell body occurs when the thickness of the lamellipodium is equal to a characteristic thickness of the cell body h_0 . Denoting the length of the lamellipodium by L , flux conservation at the transition to the cell body imposes the depolymerization velocity to be $v_d = u + v(L)$.

The solution of Eqs. (37) and (38) requires three boundary conditions. At the front of the lamellipodium, $x = 0$ the height h vanishes and there is no applied force, $F = h(\sigma - P) = 0$. At the back of the lamellipodium, $x = L$, the cell body exerts a force f_b on the lamellipodium. This force includes both the friction force on the cell body and any eventual external force applied to it. Note, that we ignore here wetting phenomena related to the advancement of the lamellipodium on the substrate and that we do not consider the surface tension forces acting on the lamellipodium.

In the middle of the lamellipodium the height is approximately constant and of order $1 \mu\text{m}$. The velocity decays then as $v(x) \simeq (-\zeta \Delta \mu / 4\eta) \exp(-x/d)$ where we have defined the velocity decay length $d^2 = 4\eta h / \xi \sim 6 \mu\text{m}$ and imposed that the stress vanishes at $x = 0$. This velocity is positive, the flow is thus in the positive x -direction and indeed corresponds to a retrograde flow. Comparing the velocity at the front with the experimental value, we obtain an estimate of the active stress $-\zeta \Delta \mu \sim 10^3$ Pa.

A numerical solution for the height profile $h(x)$, the velocity $v(x)$ and the force $F(x)$ is shown in Fig. 9. The flow is always retrograde at the front. At the back it is anterograde, if the force f_b is small. In the middle of the lamellipodium, the velocity vanishes. The lamellipodium is very flat around this point and we define its thickness as the thickness at the point where the velocity vanishes $\bar{h} = h_0 v_d / u$. If the force exerted by the cell body vanishes, $f_b = 0$, so does the total force on the lamellipodium. One can then characterize the lamellipodium by a force dipole $Q = \int dx dy \zeta v$. The explicit calculation gives $Q = A \bar{h} \zeta \Delta \mu$, where A is the area of the lamellipodium. The dipole is negative as observed experimentally for a cell on a soft substrate, which corresponds to a contractile effect of the cytoskeleton [80]. The order of magnitude of this force dipole $Q \sim -6 \times 10^{-13}$ J is consistent with the experimental data [79].

The advancing velocity of the cell is obtained from flux conservation at the back of the lamellipodium. We obtain

$$u \simeq v_d - \left(\frac{h_0}{4\eta \xi} \right)^{1/2} \left(\zeta \Delta \mu + \frac{f_b}{h_0} \right). \quad (39)$$

Remarkably, the leading term is the depolymerization velocity. The active effect due to the myosins increases the advancing velocity, but contributes only 10% to the total velocity. The dependence of the velocity as a function of the force applied at the back is complex. As might have been expected, the explicit dependence in Eq. (39) indicates a decrease of the velocity as the force increases. However, the depolymerization velocity also varies as a function of the force; in most cases, it decreases with the force as discussed in Section 2.1. Together, this could lead to a negative mobility of the cell, i.e., the velocity increases with an opposing force applied at the rear [81].

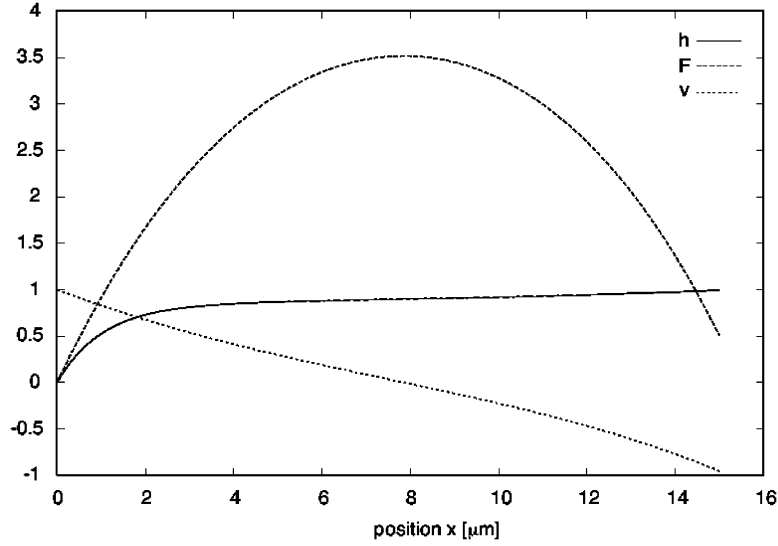


Fig. 9. Calculated velocity, force and height profiles of a thin active gel layer corresponding to a lamellipodium which moves on a substrate in the negative x -direction with velocity $u = 10 \mu\text{m}/\text{min}$. The position x is measured along the horizontal axis and given in μm . The flow velocity v of the gel layer relative to the substrate is given in $\mu\text{m}/\text{min}$, and the gel thickness h is given in μm . The integrated stress across the active gel layer F is given in units of $0.5 \text{ nN}/\mu\text{m}$. The parameter values are $\zeta\Delta\mu/4\eta = -0.21 \text{ min}^{-1}$, $\xi/4\eta = 1/(36 \mu\text{m})$, and $u = 10 \mu\text{m}/\text{min}$. Furthermore, we use $\xi = 3 \times 10^{10} \text{ Pa s/m}$ and $k_p\rho_{\text{wa}}^0 = 9 \mu\text{m}/\text{min}$.

One of the main limitations of this simple model results from our assumption of the cytoskeleton behaving as a liquid. This is certainly not true close to the front of the cell where the viscoelasticity must be taken into account. One expects a region with a length of order $u\tau$ in which the actin has a solid like behavior. The velocity in this region remains constant but a more detailed theory leads to a modified height profile in the vicinity of the front of the lamellipodium.

6.2. Relaxation modes of the cytoskeleton and wave propagation

One of the general features of active systems is the possible existence of propagating waves as has been pointed out first by Ramaswamy [20,21,24]. This has been shown for instance for active membranes or for active nematic liquids. Propagating waves have also been observed in the cytoskeleton of dictyostelium cells [82] and of spreading fibroblasts [83]. During cell spreading, lateral as well as centripetally propagating waves have been detected.

Theoretically, the existence of propagating waves in a medium can be studied by looking at the corresponding relaxation modes. A systematic study of the relaxation modes has not been performed within the framework of the linear active polar gel hydrodynamic theory. In Ref. [26], we have studied the relaxation modes of a compressible active polar gel in one dimension.

In a steady state, the actin density and the actin velocity v are constant. The velocity is imposed by actin treadmilling, $v = v_p$. Within the strictly linear theory, an active polar gel has no propagating modes. In order to have a more realistic description, we introduce explicitly two populations of myosins, myosins bound to actin at a concentration c_m and free myosins at a concentration c_u . Free myosins diffuse in the cytosol with a diffusion constant D . Bound myosins are convected by the gel movement with velocity v , but they also generate motion along the actin filaments (towards the plus-end) at a velocity v_m . This motion is due to the activity of the myosins and it is in a linear theory proportional to $\Delta\mu$. The flux of bound myosins is therefore $j_\alpha^m = c_m(v_\alpha + v_m p_\alpha)$. In comparison to the general expression of the flux given in Eq. (21), we have ignored here the diffusion of bound myosins (which correspond to fluctuations of the velocity u) and we can identify $\kappa_m\Delta\mu = c_m v_m$. The conservation equations for the two populations of myosins read

$$\partial_t c_u - D\partial_x^2 c_u = k_{\text{off}}c_m - k_{\text{on}}c_0c_u^n, \quad (40)$$

$$\partial_t c_m + \partial_x(c_m(v + v_m)) = -k_{\text{off}}c_m + k_{\text{on}}c_0c_u^n. \quad (41)$$

The attachment kinetics of the myosins to the active filaments is characterized by on- and off-rates, k_{on} and k_{off} , respectively. As bound myosins form mini-filaments, we have used here a non-linear binding kinetics with n of order 3 to 4. The active stress depends on both, the myosin density c_m and the actin density c_0 . We only consider the linear terms and define $\zeta_a = \partial_{c_0} \zeta$ as well as $\zeta_m = \partial_{c_m} \zeta$.

Investigating the relaxation of a periodic perturbations $\delta v \sim e^{ikx}$ with wave vector k around the homogeneous steady state with $v = v_p$, we obtain three modes. Two overdamped modes correspond to a chemical relaxation mode and to a chemical mode. The third is a propagating mode with a propagation speed

$$c = -\phi \left[v_0 + \frac{(\alpha c_0 + \zeta_a \Delta \mu c_0) v_m}{\alpha c_0 + \zeta_a \Delta \mu c_0 + \zeta_m c_m} \right]. \quad (42)$$

As in Section 5.2, α is the compressibility of the actin gel and ϕ the fraction of bound motors. In a cell, the total flux of bound myosins at the edge must vanish and therefore $v_m + v_p = 0$. The speed of the propagating mode is then proportional to the actin polymerization velocity and to the active coefficient ζ_m . Note, that in this polar system the modes propagate only in one direction.

6.3. Polymerization limited by active stress in a flat geometry

In many cells, actin forms a cortex just below the plasma membrane. The cortical actin controls many of the mechanical properties of the cell and is about 1 μm thick. In particular, it has recently been shown to play a major role in cell instabilities and oscillations [84,85], as well as in the transient formation of blebs by the cell membrane [86,87].

We assume here that cortical actin grows from the membrane with the plus-ends of the filaments on the membrane and the minus-ends pointing inwards. The filaments are probably almost parallel to the membrane surface and randomly oriented in the plane of the membrane. In the language of liquid crystals this corresponds to a negative nematic order parameter. Consequently, we choose the active stress to be positive, $\tilde{\zeta} \Delta \mu > 0$. With this choice and assuming an incompressible gel, the gel generates contractile stress in the plane of the membrane and under contraction increases the thickness of the gel layer.

A complete discussion of the actin cortical layer will be given in Ref. [88]. Here, we restrict our discussion to an actin layer growing from a flat membrane in the (x, y) -plane along the z direction as shown in Fig. 10.

As actin grows from the surface, the newly formed filaments are covered by myosins and the contractile stress grows. If we call τ_m^{-1} the detachment rate of the myosins from the filaments and v_p the actin polymerization velocity perpendicular to the membrane, the active stress grows as $\tilde{\zeta} \Delta \mu(z) = \bar{\zeta} \Delta \mu (1 - \exp(-z/(\tau_m v_p)))$, where $\bar{\zeta} \Delta \mu$ is the saturation value of the stress that is generated when the myosin density along the actin filaments reaches its equilibrium value. The total transverse stress $\sigma_{xx} - P$, where P is the pressure, also grows from the surface. If, for simplicity, we consider that actin depolymerization occurs only at the surface of the cortical layer, it occurs at a lateral stress $\sigma_{xx} - P$ at the gel thickness $z = h$. This increases the depolymerization rate of the gel. In the simplest Kramers approach, the depolymerization rate increases exponentially with the stress as $v_d = v_d^0 \exp\{[\sigma_{xx} - P](h)/\sigma_0\}$, where σ_0 is a stress characterizing the height of the potential barrier against depolymerization. The cortical layer therefore grows until the stress is large enough such that depolymerization exactly compensate polymerization. The thickness h of the cortical layer is thus fixed by $v_d(h) = v_p$.

If the lateral extension of the membrane is very large, the velocity field in the actin layer is oriented along the z direction and only depends on z . The incompressibility equation imposes that the velocity v_z normal to the membrane is constant. Continuity of the flux on the membrane then imposes $v_z = v_p$. Ignoring variations of the polarization module,

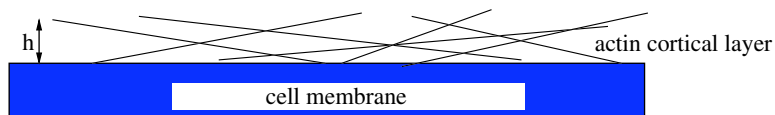


Fig. 10. Sketch of a cortical actin layer in a planar geometry. Actin polymerizes on the membrane surface and depolymerizes on the outer surface of the layer where the minus ends of the filaments are located. The actin filaments have an orientation almost parallel to the membrane surface.

the constitutive equations for the stress, Eq. (16), can be written as

$$(1 + \tau v_p \partial_z)(\sigma_{zz} + \frac{2}{3} \tilde{\zeta} \Delta \mu) = 0, \quad (43)$$

$$(1 + \tau v_p \partial_z)(\sigma_{xx} - \frac{1}{3} \tilde{\zeta} \Delta \mu) = 0. \quad (44)$$

In the following we ignore the variation of the modulus p of the polarization vector. We have supposed in Eq. (43) that this modulus is equal to 1. If it is different from 1, the active stress must be multiplied by \mathbf{p}^2 according to Eq. (16). Force balance in the z -direction imposes $\partial_z(\sigma_{zz} - P) = 0$. Taking the boundary condition at the free surface into account, this implies $\sigma_{zz} = P$. The boundary condition for the stress σ_{xx} on the membrane, at $z=0$, depends on the state of the active gel when it polymerizes. The simplest polymerization condition is given by $(\sigma_{xx} - P)(z=0) = 0$, that is the gel is stress free when it polymerizes. In this case, the stress on the surface is $(\sigma_{xx} - P)(h) = (\tilde{\zeta} \Delta \mu)(h)$ at $z = h$ and the steady-state thickness of the cortical actin layer is given by

$$h = -v_p \tau_m \log \left(1 - \frac{g \sigma_0}{\tilde{\zeta} \Delta \mu} \right), \quad (45)$$

where $g = \log v_p / v_d^0$ is a dimensionless polymerization free energy. If the active stress is very large the cortical actin layer is very thin. When $\tilde{\zeta} \Delta \mu = g \sigma_0$, the thickness of the actin layer diverges and the cortical layer invades all the cytoplasm. However, in this case, the actin monomer diffusion through the cortical layer must be taken into account, which fixes the thickness of the cortical layer.

In a next step, the stability of the cortical actin layer should be studied, see [88], where this analysis is performed for a cortical layer in a spherical geometry mimicking a cell. For a broad range of parameters, the cortical layer is unstable. Such cortical instabilities could be related to oscillatory instabilities of cells [85]. Furthermore, cortical instabilities could be related to the formation of blebs, when the cortical gel fails to stabilize the membrane geometry and membrane vesicles bud off the cell [87]. Pattern formation in the cortex has also been discussed in cylindrical geometry based on an effective two-dimensional description of an active gel layer close to a surface [89]. This description is derived from more microscopic models of filament interactions near a surface and can be viewed as a simplified two-dimensional projection of the cortical layer discussed here.

7. Concluding remarks

In the preceding sections, we have shown how a macroscopic hydrodynamic theory can account for mechanical properties of the cytoskeleton in living cells as well as for purified subsystems of the cytoskeleton studied in vitro. The macroscopic properties of the cytoskeleton essentially follow from its symmetries and its inherent activity. The symmetries are comprehensively captured by describing the cytoskeleton as a polar physical gel. The activity is due to processes driven by ATP hydrolysis, like the action of molecular motors or the assembly and disassembly of filaments in presence of cross-linking proteins. Based on these properties, the hydrodynamic theory is obtained by following the same approach as Martin, Parodi, and Pershan for describing the dynamics of condensed matter on large length and time scales [16]. The important new ingredient, which captures the activity of the cytoskeleton, is the generalized force due to differences $\Delta \mu$ in the chemical potentials of ATP and its hydrolysis products. As we have seen, the activity not only modifies the bulk material properties: treadmilling leads to unique boundary conditions in elasticity problems of the cytoskeleton.

The hydrodynamic equations depend on a set of phenomenological parameters such as viscosities and elastic moduli. Most of these parameters are known from liquid crystal physics and experiments have been devised to measure them. For actin gels, however, the values of many of these parameters are unknown, for example, the rotational viscosity γ_1 or the coupling between polarization and stress v_1 . The same is true for the new parameters connected to the activity of the material. As the other Onsager coefficients, they are material parameters and new experimental setups have to be devised to measure them. Considering the cytoskeleton as being incompressible, there is really only one new parameter, $\tilde{\zeta}$, coupling the activity measured by $\Delta \mu$ to the stress in the system. While direct measurements of this value have not yet been performed, the corresponding active stress can be estimated for lamellipodia of keratocytes. To this end the results of the analysis presented in Section 6.1 are compared to measurements on keratocytes. This yields a value of $-\zeta \Delta \mu = 10^3$ Pa. Applying the same approach to neuronal growth cones, the value seems to be slightly smaller [90].

Since the hydrodynamic theory is based on symmetries only, the theory of active polar gels can be applied to any active system with polar order. In addition to the acto-myosin system, these include microtubules interacting with kinesin or dynein motors, but also colonies of swimming bacteria or cellular tissues (in many tissues cells are polarized). Furthermore, flocks of birds and fish schools fall into this class and an approach similar to the one presented here has been used for their description. Note that in contrast to the cytoskeleton, inertial effects cannot be neglected in the latter cases. Being described by the same equations, the values of the phenomenological coefficients differ from system to system. As stated above, they can be measured directly. Another way is to consider microscopic models which in simple limits can be related to the hydrodynamic theory [14,15,50,91–93]. Using such models, the phenomenological parameters can be estimated from single molecule properties.

The physics of active systems is only at its beginning and the introduction of activity in the hydrodynamic equations leads to many new physical effects. We have given here a few examples of spontaneous flow and instabilities driven by the activity. There is still a long way to go before the consequences of these effects for cellular behavior have been fully explored. It is remarkable, though, that already the one-component theory for systems close to thermodynamic equilibrium analyzed in simple geometries can qualitatively account for phenomena such as the retrograde flow in crawling cells or the height profile of lamellipodia. A quantitative description of these effects in cellular systems likely requires to explicitly consider several components and to go beyond the linear theory presented here. Unlike the linear theory reviewed in this work, however, there is no systematic way to build this more general theory. Therefore an intense and systematic cross-talk between experiments and theory will be needed.

Acknowledgments

We would like to thank our coworkers for this work, K. Sekimoto (University Paris VII), R. Voituriez (University Paris VI), E. Paluch (Dresden), P. Dewimille, G. Salbreux and A. Zumdick (Institut Curie) and A. Basu (Calcutta). We also acknowledge support of the European Commission through the European network “Phyneys” (HPRN-CT-2002-00312).

References

- [1] B. Alberts, et al., *Molecular Biology of the Cell*, fourth ed., Garland, New York, 2002.
- [2] D. Bray, *Cell Movements*, second ed., Garland, New York, 2001.
- [3] J. Howard, *Mechanics of Motor Proteins and the Cytoskeleton*, Sinauer Associates Inc., Sunderland, 2001.
- [4] C. Revenu, R. Athman, S. Robine, D. Louvard, *Nat. Rev. Mol. Cell. Biol.* 5 (2004) 635.
- [5] P.G. De Gennes, *Scaling Concepts in Polymer Physics*, Cornell University Press, Ithaca, 1985.
- [6] D.A. Head, A.J. Levine, F.C. MacKintosh, *Phys. Rev. Lett.* 91 (2003) 108102.
- [7] J. Wilhelm, E. Frey, *Phys. Rev. Lett.* 91 (2003) 108103.
- [8] A.B. Verkhovskiy, T.M. Svitkina, G.G. Borisy, *Curr. Biol.* 9 (1999) 11.
- [9] K. Takiguchi, *J. Biochem.* 109 (1991) 520.
- [10] Y. Tanaka-Takiguchi, T. Kakei, A. Tanimura, A. Takagi, M. Honda, H. Hotani, K. Takiguchi, *J. Mol. Biol.* 341 (2004) 467.
- [11] K. Kruse, F. Jülicher, *Phys. Rev. Lett.* 85 (2000) 1778.
- [12] K. Kruse, S. Camalet, F. Jülicher, *Phys. Rev. Lett.* 87 (2001) 138101.
- [13] K. Kruse, F. Jülicher, *Phys. Rev. E* 67 (2003) 051913.
- [14] T.B. Liverpool, M.C. Marchetti, *Phys. Rev. Lett.* 90 (2003) 138102.
- [15] A. Ahmadi, T.B. Liverpool, C.M. Marchetti, *Phys. Rev. E* 72 (2005) 060901.
- [16] P.C. Martin, O. Parodi, P. Pershan, *Phys. Rev. A* 6 (1972) 2401.
- [17] K. Sekimoto, *J. Phys. II (France)* 1 (1991) 19.
- [18] J.-B. Manneville, P. Bassereau, S. Ramaswamy, J. Prost, *Phys. Rev. E* 64 (2001) 021908.
- [19] I.S. Aranson, L.S. Tsimring, *Rev. Mod. Phys.* 78 (2006) 641.
- [20] R.A. Simha, S. Ramaswamy, *Phys. Rev. Lett.* 89 (2002) 058101.
- [21] Y. Hatwalne, S. Ramaswamy, M. Rao, R.A. Simha, *Phys. Rev. Lett.* 92 (2004) 118101.
- [22] C. Dombrowski, L. Cisneros, S. Chatkaew, R.E. Goldstein, J.O. Kessler, *Phys. Rev. Lett.* 93 (2004) 098103.
- [23] J. Toner, Y. Tu, *Phys. Rev. Lett.* 75 (1995) 4326.
- [24] S. Ramaswamy, J. Toner, J. Prost, *Phys. Rev. Lett.* 84 (2000) 3494.
- [25] K. Kruse, J.F. Joanny, F. Jülicher, J. Prost, K. Sekimoto, *Phys. Rev. Lett.* 92 (2004) 078101;
K. Kruse, J.F. Joanny, F. Jülicher, J. Prost, K. Sekimoto, *Phys. Rev. Lett.* 93 (2004) 099902 erratum
- [26] K. Kruse, J.F. Joanny, F. Jülicher, J. Prost, K. Sekimoto, *Eur. Phys. J. E* 16 (2005) 5.
- [27] J. Prost, in: H. Flyvbjerg, F. Jülicher, P. Ormos, F. David (Eds.), *Physics of Bio-molecules and Cells*, EDP Sciences, Les Ulis, 2001, pp. 215–236.

- [28] A. Bernheim-Groswasser, S. Wiesner, R. Golsteyn, M.F. Carlier, C. Sykes, *Nature* 417 (2002) 308.
- [29] M.F. Carlier, S. Wiesner, C. Le Clainche, D. Pantaloni, C. R. Biology 326 (2003) 161.
- [30] H. Boukellal, O. Campas, J.F. Joanny, J. Prost, C. Sykes, *Phys. Rev. E* 69 (2004) 061906.
- [31] A. Upadhyaya, J. Chabot, A. Andreeva, A. Samadani, A. van Oudenaarden, *Proc. Nat. Acad. Sci. USA* 100 (2003) 4521.
- [32] P.A. Giardini, D.A. Fletcher, J.A. Theriot, *Proc. Nat. Acad. Sci. USA* 100 (2003) 6493.
- [33] K. Sekimoto, J. Prost, F. Jülicher, H. Boukellal, A. Bernheim-Groswasser, *Eur. Phys. J. E* 13 (2004) 247.
- [34] J. Van der Gucht, E. Paluch, J. Plastino, C. Sykes, *Proc. Nat. Acad. Sci. USA* 102 (2005) 5847.
- [35] E. Paluch, Ph.D. Thesis, University Paris VI, 2005.
- [36] R.B. Bird, R.C. Armstrong, Curtiss, *Dynamics of Polymeric Liquids*, second ed., Wiley, New York, 1987.
- [37] R. Larson, *Constitutive Equations for Polymer Melts and Solutions*, Butterworth-Heinemann, 1998.
- [38] F. Wottawah, S. Schinkinger, B. Lincoln, R. Ananthakrishnan, M. Romeyke, J. Guck, J. Käs, *Phys. Rev. Lett.* 94 (2005) 098103.
- [39] H.A. Kramers, *Physica (Utrecht)* 7 (1940) 284.
- [40] J. Plastino, J. Lelidis, J. Prost, C. Sykes, *Eur. Biophys. J.* 33 (2004) 310.
- [41] U. Euteneuer, M. Schliwa, *Nature* 310 (1984) 58.
- [42] A. Bershadsky, M. Kozlov, B. Geiger, *Curr. Opin. Cell Biol.* 18 (2006) 1.
- [43] K. Tawada, K. Sekimoto, *J. Theor. Biol.* 150 (1999) 192.
- [44] P.G. De Gennes, J. Prost, *The Physics of Liquid Crystals*, Clarendon Press, Oxford, 1993.
- [45] B. Fabry, G.N. Maksym, J.P. Butler, M. Glogauer, D. Navajas, J. Fredberg, *Phys. Rev. Lett.* 87 (2001) 148102.
- [46] M. Balland, N. Desprat, D. Icard, S. Fereol, A. Asnacios, J. Browaeys, S. Henon, F. Gallet, *Phys. Rev. E* 74 (2006) 021911.
- [47] H.Y. Lee, M. Kardar, *Phys. Rev. E* 64 (2001) 056113.
- [48] J. Kim, Y. Park, B. Kahng, H.Y. Lee, *J. Korean Phys. Soc.* 42 (2003) 162.
- [49] S. Sankararaman, G.I. Menon, P.B. Kumar, *Phys. Rev. E* 70 (2004) 031905.
- [50] I.S. Aronson, L.S. Tsimring, *Phys. Rev. E* 71 (2005) 050901(R).
- [51] M. Doi, S.F. Edwards, *The Theory of Polymer Dynamics*, Oxford University Press, Oxford, 1986.
- [52] M. Warner, E.M. Terentjev, *Liquid Crystal Elastomers*, Oxford University Press, Oxford, 2003.
- [53] P. Stein, N. Assfalg, H. Finkelmann, P. Martinoty, *Eur. Phys. J. E* 4 (2001) 255.
- [54] P. Dewimille, Ph.D. Thesis University Paris VI, 2006.
- [55] J.F. Joanny, F. Jülicher, K. Kruse, J. Prost, *Hydrodynamic Theory for Multi-component Active Viscoelastic Polar Fluids*, 2006, in preparation.
- [56] A. Mogilner, G. Oster, *Biophys. J.* 84 (2003) 1591.
- [57] E. Evans, P. Williams, in: H. Flyvberg, F. Jülicher, P. Ormos, F. David (Eds.), *Physics of Biomolecules and Cells*, EDP Sciences, Les Ulis, 2001, pp. 145–204.
- [58] A. Basu, J.F. Joanny, F. Jülicher, J. Prost, *Stochastic Dynamics of Visco-elastic Active Polar Gels*, 2006, in preparation.
- [59] N. Gov, *Phys. Rev. Lett.* 93 (2004) 268104.
- [60] B. Nadrowski, P. Martin, F. Jülicher, *Proc. Nat. Acad. Sci. USA* 101 (2004) 12195.
- [61] R. Voituriez, J.F. Joanny, J. Prost, *Eur. Phys. Lett.* 70 (2005) 404.
- [62] S. Ramaswamy, private communication, 2006.
- [63] F.J. Nédélec, T. Surrey, A.C. Maggs, S. Leibler, *Nature* 389 (1997) 305.
- [64] T. Surrey, M.B. Elowitz, P.-E. Wolf, F. Yang, F. Nédélec, K. Shokat, S. Leibler, *Proc. Natl. Acad. Sci. USA* 95 (1998) 4293.
- [65] F.J. Nédélec, T. Surrey, A.C. Maggs, *Phys. Rev. Lett.* 86 (2001) 3192.
- [66] T. Surrey, F. Nédélec, S. Leibler, E. Karsenti, *Science* 292 (2001) 1167.
- [67] D. Smith, F. Ziebert, D. Humphrey, C. Duggan, W. Zimmermann, J. Käs, *Molecular Motor-induced Instabilities and Crosslinkers Determine Biopolymer Organization*, *Biophys. J.* (2006), submitted.
- [68] R. Voituriez, J.F. Joanny, J. Prost, *Phys. Rev. Lett.* 96 (2006) 028102.
- [69] S. Higashi-Fujime, *J. Cell Biol.* 101 (1985) 2335.
- [70] A. Szent-Gyorgyi, *Chemistry of Muscle Contraction*, Academic Press, New York, 1947 & 1951.
- [71] G.A. Hinshaw Jr., R.G. Petschek, R.A. Pelcovits, *Phys. Rev. Lett.* 60 (1988) 18.
- [72] D. Blankschtein, R.M. Hornreich, *Phys. Rev. B* 32 (1985) 3214.
- [73] P. Valloton, et al., *Mol. Biol. Cell* 16 (2005) 1223.
- [74] K. Kruse, J.F. Joanny, F. Jülicher, J. Prost, *Phys. Biol.* 3 (2006) 130.
- [75] T.D. Pollard, G.G. Borisy, *Cell* 112 (2003) 453.
- [76] M.F. Carlier, D. Pantaloni, *J. Mol. Biol.* 269 (1997) 459.
- [77] S.M. Rafelski, J.A. Theriot, *Ann. Rev. Biochem.* 73 (2004) 209.
- [78] A. Carlsson, *Biophys. J.* 81 (2001) 1907.
- [79] T. Oliver, M. Dembo, K. Jacobson, *J. Cell. Biol.* 145 (1999) 589.
- [80] I. Bischofs, S. Safran, U. Schwarz, *Phys. Rev. E* 69 (2004) 021911.
- [81] J.F. Joanny, F. Jülicher, J. Prost, *Phys. Rev. Lett.* 90 (2003) 168102.
- [82] T. Bretschneider, S. Diez, K. Anderson, J. Heuser, M. Clarke, A. Müller-Taubenberger, J. Kohler, G. Gerisch, *Curr. Biol.* 14 (2004) 1.
- [83] G. Giannone, B.J. Dubin-Thaler, H.G. Döbereiner, N. Kieffer, A.R. Bresnick, M.P. Sheetz, *Cell* 116 (2004) 431.
- [84] O. Pletjushkina, Z. Rajfur, P. Pomorski, T. Oliver, J. Vasiliev, K.A. Jacobson, *Cell Motil. Cytoskel.* 48 (2001) 235.
- [85] E. Paluch, M. Piel, J. Prost, M. Bornens, C. Sykes, *Biophys. J.* 89 (2005) 724.
- [86] J. Dai, M.P. Sheetz, *Biophys. J.* 77 (1999) 3363.
- [87] G.T. Charras, J.C. Yarrow, M.A. Horton, L. Mahadevan, T.J. Mitchison, *Nature* 435 (2005) 365.

- [88] G. Salbreux, J.F. Joanny, J. Prost, Instabilities of Cortical Actin Layers (2006), in preparation.
- [89] A. Zumdieck, M.C. Lagomarsino, C. Tanase, K. Kruse, B. Mulder, M. Dogterom, F. Jülicher, *Phys. Rev. Lett.* 95 (2005) 258103.
- [90] T. Betz, D. Lim, J.A. Käs, *Phys. Rev. Lett.* 96 (2006) 098103.
- [91] K. Kruse, A. Zumdieck, F. Jülicher, *Europhys. Lett.* 64 (2003) 716.
- [92] F. Ziebert, W. Zimmermann, *Eur. Phys. J. E* 17 (2005) 41.
- [93] K. Kruse, F. Jülicher, *Eur. Phys. J. E* 20 (2006) 459.
- [94] F. Backouche, L. Haviv, D. Groswasser, A. Bernheim-Groswasser, *Phys. Biol.* 3 (2006) 264.